

**POST PROCESSING TECHNIQUES OF 3D PRINTED PART AND ITS EFFECTS ON
MECHANICAL PROPERTIES**



UNIVERSITI TEKNIKAL MALAYSIA MELAKA

**POST PROCESSING TECHNIQUES OF 3D PRINTED PART AND ITS EFFECTS
ON MECHANICAL PROPERTIES**

LEONG KOK SENG

**The thesis is submitted in fulfillment of the requirements for the Bachelor of
Mechanical Engineering**



UNIVERSITI TEKNIKAL MALAYSIA MELAKA

2018

DECLARATION OF ORIGINAL WORK

I hereby declare that this thesis entitled “Post Processing Techniques of 3D Printed Part and Its Effects on Mechanical Properties” is the result of my own, except as cited in the references. The thesis has not been accepted for any degree and is not concurrently submitted in candidature of any other degree.



SIGNATURE : _____
NAME : LEONG KOK SENG
DATE : 16th MAY 2018

اونيورسيتي تيكنيكل مليسيا ملاك

UNIVERSITI TEKNIKAL MALAYSIA MELAKA

SUPERVISOR'S APPROVAL

‘ I, hereby declared that I had read through this thesis and in my opinion that this thesis is adequate in terms of scope and quality which fulfill the requirements for the award of Bachelor of Mechanical Engineering.’

SIGNATURE : _____
NAME OF SUPERVISOR : IR. DR. MOHD RIZAL BIN ALKAHARI
DATE : _____



DEDICATION

I would like to dedicate the appreciation to my parents, Leong Soon Chee and Ching Chooi Fong who supported me from spiritually and financially, my supervisor, Ir. Dr. Mohd Rizal bin Alkahari and my course mates that assisted me through the journey of research.



ABSTRACT

Fused Deposition Modeling (FDM) is one of the additive manufacturing technology, where printing material is deposited layer by layer onto the surface to form a complex product. FDM technique is widely used in producing prototypes. However, FDM technique has poor surface finishing and staircase effect compared to other additive manufacturing techniques. The purpose of this study was to develop a new post-treatment technique, known as Blow Cold vapor smoothing treatment. Later analysis on the effectiveness of this newly developed post-treatment technique and evaluate the tensile strength of the printed part. The specimens were printed using open source low-cost 3D printer with acrylonitrile-butadiene-styrene (ABS) printing material. Acetone solvent was used in this Blow Cold vapor smoothing treatment. A comparison in term of surface roughness value and tensile strength was made between the treated and untreated specimens. It was found that the surface roughness value on the treated specimen was reduced dramatically. However, this post-treatment technique weaken the material structure of the outer layer on the specimen, which had a slight effect on the tensile strength of the specimen.

ABSTRAK

Fused Deposition Modeling (FDM) atau dikenali sebagai proses pembuatan pertambahan adalah proses untuk membuat objek berbentuk 3 dimensi dari model digital dengan menggunakan teknik membuat objek daripada sejumlah bahan plastik dicetak berlapis-lapis di bawah kawalan komputer sehingga membentuk objek yang diinginkan. Walau bagaimanapun, produk hasil daripada teknik FDM mempunyai permukaan yang lebih kasar dan kesan staircase berbanding dengan teknik yang lain. Kajian ini bertujuan untuk menghasilkan satu proses baru untuk melicinkan permukaan spesimen selepas cetakan. Seterusnya, menganalisis kesan keberkesanan teknik ini dan menilaikan kekuatan spesimen selepas menggunakan teknik rawatan ini. Teknik rawatan ini dikenali sebagai teknik Blow Cold vapor smoothing. Spesimen dicetak dengan menggunakan 3D printer yang kos rendah dan perisian sumber terbuka. Sumber bahan plastik cetakan yang digunakan adalah plastik acrylonitrile-butadiene-styrene (ABS). Pelarut kimia yang digunakan dalam teknik rawatan Blow Cold vapor smoothing adalah aseton. Perbandingan dibuat dari segi kekasaran permukaan dan kekuatan spesimen antara spesimen sebelum dan selepas rawatan. Hasil perbandingan menunjuk bahawa kekasaran permukaan selepas rawatan menurun secara dramatik, tetapi teknik rawatan ini akan melemahkan struktur bahan pada lapisan spesimen yang paling luar. Oleh sebab itu, kekuatan spesimen akan mengurang sedikit.

ACKNOWLEDGEMENTS

First and foremost, I would like to take this opportunity to express my sincere acknowledgment to my supervisor Ir. Dr. Mohd Rizal bin Alkahari from Faculty of Mechanical Engineering Universiti Teknikal Malaysia Melaka (UTeM) for his essential supervision, support and encouragement towards the completion of this thesis. His timely advice, meticulous scrutiny, and scholarly advice had helped me to a very great extent to accomplish this thesis.

I would also like to express my gratitude to Professor Dr. Ghazali bin Omar, the person in charge for Advanced Materials Characterization Laboratory (AMCHAL) Faculty of Mechanical Engineering, Mr. Azrul Syafiq bin Mazlan, the technician from Tribology laboratory Faculty of Mechanical Engineering, Madam Adybah Atyqa Shahrina binti Aimee Shah, technician from Chemical laboratory Faculty of Mechanical Engineering, and Mr. Mohd Yuszrin bin Md Yacob, technician from Final Year Project (PSM) laboratory for their kind assistant and efforts in all the labs and analysis works. Special thanks profusely to UTeM for the financial support throughout this study.

I am extremely thankful to my mentor, Siti Nur Humaira binti Mazlan for her overwhelming guidance throughout this study. I also do not forget to thank all my peers, friends, family and all who, directly or indirectly have lent their helping hand throughout this study.

TABLE OF CONTENTS

	PAGE
DECLARATION OF ORIGINAL WORK	
DEDICATION	
ABSTRACT	i
ABSTRAK	ii
ACKNOWLEDGEMENT	iii
TABLE OF CONTENTS	iv
LIST OF TABLES	vii
LIST OF FIGURES	ix
LIST OF ABBREVIATIONS	xi
LIST OF APPENDICES	xii
CHAPTER	
1. INTRODUCTION	1
1.1 Background	1
1.2 Problem Statement	2
1.3 Objectives	3
1.4 Scopes of Project	3
2. LITERATURE REVIEW	4
2.1 Rapid Prototyping	4
2.1.1 Additive Manufacturing (AM)	6
2.1.2 Subtractive Manufacturing	8
2.2 Classification of Additive Manufacturing	9
2.3 Fused Deposition Modeling (FDM)	12
2.3.1 Open Source Fused Deposition Modeling (FDM)	12

2.3.2	Working Principle of Fused Deposition Modeling (FDM)	13
2.3.3	Advantages of Fused Deposition Modeling (FDM)	14
2.3.4	Disadvantages of Fused Deposition Modeling (FDM)	15
2.3.5	Printing Material for Fused Deposition Modeling (FDM)	15
2.3.5.1	Acrylonitrile Butadiene Styrene (ABS)	16
2.3.5.2	Polylactic Acid (PLA)	16
2.4	Introduction on Blow Cold Vapor Smoothing Treatment	17
3.	METHODOLOGY	19
3.1	Introduction	19
3.2	Open Source FDM Printer	19
3.3	Working Procedure of Fused Deposition Modeling (FDM)	20
3.3.1	FDM Pre-Process	20
3.3.2	FDM Post-Process	22
3.4	Project Specimen	23
3.5	Apparatus	24
3.5.1	Shimadzu Ag10kNX Universal Testing Machine	24
3.5.2	Shodensha GR3400 3D Non-Contact Profilometer	24
3.5.3	Blow Cold Vapor Treatment Chamber	24
3.5.4	Acetone	26
3.6	Location	26
3.7	Design of Experiment	26
3.7.1	Taguchi Method	27
3.8	Flow Chart	31
4.	RESULTS AND ANALYSIS	32
4.1	Blow Cold Vapor Smoothing Chamber	32
4.2	Process Parameters	35
4.3	Surface Roughness	37
4.4	Blow Cold Vapor Smoothing Treatment	42
4.5	Tensile Strength	50

5. CONCLUSION AND RECOMMENDATION	55
5.1 Justification of Objectives	55
5.2 Review of Methods	55
5.3 Review of Significant Findings	56
5.4 Explanation of Significance Findings	57
5.5 Limitation of the Study	58
5.6 Implications of the Study	58
5.7 Recommendations for Future Studies	58
REFERENCES	59
APPENDICES	66



LIST OF TABLES

TABLE	TITLE	PAGE
3.1	FDM Printer Specification	19
3.2	Specification of Blow Cold Vapor Treatment Chamber	25
3.3	Chemical Properties of Acetone	26
3.4	Experiment Location	26
3.5	Taguchi Orthogonal Array	30
4.1	Blow Cold Vapor Smoothing Treatment Container Specification	33
4.2	Acetone Container Specification	33
4.3	Comparison between 4 Different Sealants and Its Ability to Resist Corrosion.	34
4.4	Fixed Parameters throughout the Experiment	36
4.5	Printing Parameters and Its Level	36
4.6	Experimental Result for Surface Roughness Value at Three Different Spots	37
4.7	Physical Appearance and Surface Profile of the 3D Printed Part	38
4.8	Experimental Result for Surface Roughness and S/N ratio	40
4.9	S/N Ratio Corresponding to Process Parameters and Its Level	41
4.10	Blow Cold Vapor Smoothing Parameter Conditions for 20 ml Acetone	43
4.11	Measured Surface Roughness Value against Exposure Time for 20 ml Acetone	43
4.12	Surface Profile of the Specimens (20 ml Acetone)	44

TABLE	TITLE	PAGE
4.13	Ratio Factor to Determine Amount of Acetone Needed	45
4.14	Blow Cold Vapor Smoothing Parameter Conditions for 23.5 ml Acetone	45
4.15	Measured Surface Roughness Value against Exposure Time for 23.5 ml Acetone	46
4.16	Surface Profile of the Specimens (23.5 ml Acetone)	48
4.17	Optical Image of the Specimens (23.5 ml Acetone)	49
4.18	Tensile Test Parameters Condition	50
4.19	Tensile Strength of the Specimens	52



LIST OF FIGURES

FIGURE	TITLE	PAGE
2.1	Product Development Cycle	5
2.2	Fused Deposition Modeling Process	6
2.3	Complex Air Duct System Used in Aerospace Industry Fabricate by Additive Manufacturing Process	7
2.4	Conceptual Comparison between Subtractive and Additive Manufacturing	7
2.5	Subtractive Manufacturing – Milling process	9
2.6	Classification of Processes According to Material State Technique	10
2.7	Classification of Processes According to Shape Building Technique	11
2.8	Fused Deposition Modeling	12
2.9	First RepRap Project – Darwin	13
2.10	FDM Working Principle	14
2.11	Farming Equipment	15
2.12	Vapor Smoothing Technique	17
2.13	Blow Cold Vapor Smoothing Treatment	18
3.1	Geeetech Prusa I3	20
3.2	3D Modeling Generated using Catia CAD Software	21
3.3	Repetier Software	21
3.4	Pronterface Software	22
3.5	Different Post-Processing Methods	22
3.6	Vapor Smoothing	23
3.7	Dogbone-shaped Test Specimen	24

FIGURE	TITLE	PAGE
3.8	Shimadzu Ag10kNX Universal Testing machine	24
3.9	Shodensha GR3400 3D Non-Contact Profilometer	25
3.10	Process Factors and Response	27
3.11	Flow Chart	31
4.1	Blow Cold Vapor Smoothing Treatment Container	32
4.2	Acetone Container	33
4.3	Acetone Corrosion Resistibility Experiment	34
4.4	Blow Cold Vapor Smoothing Treatment Container	35
4.5	Acetone Container	35
4.6	Surface Roughness Measuring Spots	37
4.7	Main Effect Plot for Means	41
4.8	Main Effect Plot for S/N Ratio	41
4.9	Blow Cold Vapor Smoothing Process	43
4.10	Graph of Average Surface Roughness against Exposure Time	44
4.11	Graph of Surface Roughness Value against Exposure Time for 23.5 ml Acetone	46
4.12	Dogbone Specimen	47
4.13	Tensile Test Specimen's Specification	51
4.14	Universal Testing Machine	51
4.15	Stress – Strain Curve	52
4.16	Graph of Tensile Strength against Exposure Time	53
4.17	Cross Section of Dogbone Specimen	54

LIST OF ABBREVIATIONS

3D	3 Dimensional
FDM	Fused Deposition Modeling
MEK	Methyl Ethyl Ketone
RTV	Room-Temperature-Vulcanizing
UTeM	Universiti Teknikal Malaysia Melaka
UV	Ultraviolet



LIST OF APPENDICES

APPENDIX	TITLE	PAGE
A	Specimen Dimension ASTM D368 Type I	66
B	Blow Cold Vapor Smoothing Treatment Chamber Assembly Drawing	67
C	Blow Cold Vapor Smoothing Treatment Chamber Orthographic Drawing	68
D	Blow Cold Vapor Smoothing Treatment Chamber Orthographic Drawing (Back Side)	69
E	Acetone Container Assembly Drawing (Front Side)	70
F	Acetone Container Assembly Drawing (Back Side)	71
G	Acetone Container Orthography View	72

CHAPTER 1

INTRODUCTION

1.1 BACKGROUND

Rapid Prototyping is defined as a collective method used to quickly design and create a scaled size model or part using three-dimension computer-aided design (CAD) software data. With the help of Rapid Prototyping technology, prototypes are able to produce quicker and in a more effective way. Rapid Prototyping technology is a time-saving technique to fabricate complexly shaped prototype by using additive manufacturing method. 3D printing is also known as additive manufacturing. Additive manufacturing is a process of designing a solid prototype using computer-aided design software, converting the designed solid into Standard Triangulation Language (STL) format and fabricating the designed solid using 3D printer. Stereolithography (SLA) method is an early and most widely used technology developed by 3D Systems of Valencia, CA, USA in 1986 (Gibson and Bártolo, 2011).

There are a few different methods of 3D printing, but Fused Deposition Modeling (FDM) is most widely used process (Palermo, 2013). FDM technique was developed and patented by Scott Crump and Lisa Crump, co-founder of Stratasys, Ltd. in 1988 (Anonymous, 2013). The FDM processes are filament first being extruded by the filament extruder, then, the filament is heated to the semi-molten temperature, and the semi-molten filament is flowing out through the automatic controlled nozzle depositing material layer by layer onto the surface (Conner et al., 2014). The printing materials which are most widely used include Polylactic acid (PLA) and Acrylonitrile butadiene styrene (ABS). However, the

disadvantage of using FDM additive method is high surface roughness compare with other methods (Krolczyk, Raos, and Legutko, 2014).

Two most important criteria of a product in many engineering industries are surface roughness and surface topography (Poljacek et al., 2008). Surface roughness treatment can be classified into two methods; Pre-processing method and Post-processing method. In pre-processing method, optimum printing parameters such as layer thickness, raster angle, infill density, infill pattern, nozzle temperature are determined to maximize the mechanical properties of the project. However, “staircase” effect still can be found on the surface and greatly influence the surface roughness. Post-processing methods such as sanding, chemical treatment, painting are needed to reduce the staircase effect and improve the surface roughness.

In this study, a new post-processing method, namely Blow Cold vapor smoothing treatment was proposed. Previous researches had done using post-processing hot acetone vapor bath method was proved to be very effective in improving the surface roughness. However, this process was dangerous due to acetone is highly flammable. This new post-processing method was practically safe which does not involve heating the acetone.

1.2 PROBLEM STATEMENT

3D printing technology is an emerging technology and widely used in producing prototyping. Many researches and studies have been done to enhance the functionality and improve the mechanical properties of the 3D printed project. FDM technique is one of the widely used 3D printing technology. However, FDM technique has higher surface roughness value compare to other techniques. One of the key factors that influences the surface roughness of the FDM printed part was temperature (Chaidas et al., 2016). As the temperature increases, the filament material was tended to liquefy to a more liquid stage and

hence, softening the printed surface (Bharath, Dharma, and Henderson, 2000). This will result in lowering its flexural modulus. As the new layer is printed, the previous layer will tend to curve downward and results in preferential flow and reduce surface finish (Comb, Priedeman, and Turley, 1994). Therefore, optimum temperature needs to be determined using Taguchi method. Besides that, a new post-processing method needs to be researched in order to further improve the surface roughness of the part produced by FDM technique.

1.3 OBJECTIVES

The objectives of this study are as follows:

- i) To analyze effectiveness of post treatment process.
- ii) To evaluate the mechanical properties of the treated 3D printed part.
- iii) To study the optimum parameter in post process method.

1.4 SCOPES OF PROJECT

The scopes of this project are:

- i) Fabrication was made using low cost 3D printer (Open source system / entry level printer).
- ii) Acetone was used as chemical agent.
- iii) The project used thermoplastic material such as ABS material.

CHAPTER 2

LITERATURE REVIEW

2.1 Rapid Prototyping

“Prototyping” is defined as the product development in term of shape, dimension and functionality of a designed part before investment in large-scale manufacturing process (Pham and Gault, 1998). In term of marketing, prototype is the physical model which able to present the design concept, idea, functionality of a product to the customers and modifications can be made to meet customers’ requirements (Yan and Gu, 1996). In term of engineering, prototype able to help engineers to transform the CAD data into physical model, which helps to visualize exactly the actual product (Yan and Gu, 1996). This is useful for engineers to anticipate the problem while designing the complex part.

Campbell et al. (2012) defined rapid prototyping as “a wide range of technologies that fabricate prototypes, layer by layer in a quick and automated manner during the early stages of product development”. One of the advantages in rapid prototyping is able to produce the physical model with range of automated technologies and validate the product rapidly with minimum cost. Therefore, design changes can be happened in the earlier stages of product development and reduce the amendment’s cost at the later stages (Gurr and Mülhaupt, 2012). Figure 2.1 below shows the flowchart of product development cycle. Studies proved that rapid prototyping able to reduce product development cost by up to 70% and time to market by 90% (Pham and Gault, 1998).

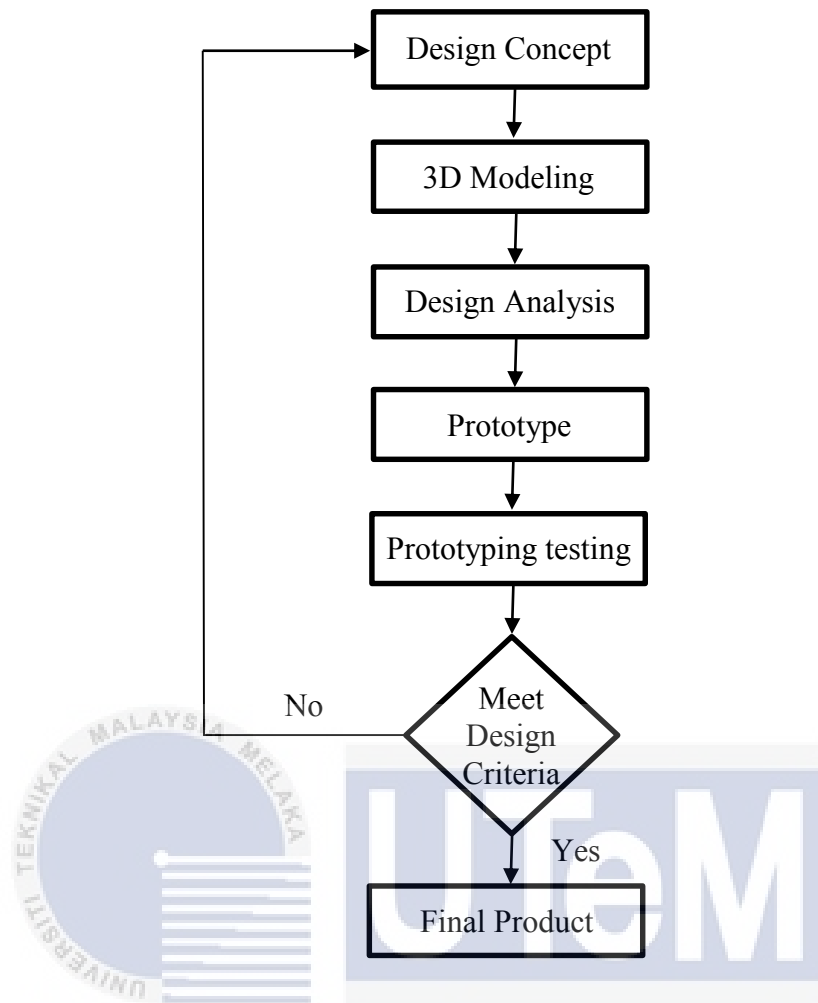


Figure 2.1: Product Development Cycle (Wong and Hernandez, 2012).

Gurr (2012) explained rapid prototyping synonymously demoted as “solid freeform fabrication (SFF) or layered manufacturing (LM), represents layer by layer fabrication of 3-dimensional (3D) prototypes”. All the preprocessing procedures are almost same throughout all the rapid prototyping process. The 3D modeling data of the prototype is created by computer-aided design (CAD) software or 3D scanning, and sliced into layers to obtain information needed for producing the 3D product. Rapid prototyping technologies can be divided into additive manufacturing and subtractive manufacturing.

2.1.1 Additive Manufacturing (AM)

Additive manufacturing is defined as “the process of joining materials to make object from three dimensional (3D) model data, usually layer upon layer as opposed to subtractive manufacturing methodologies” (Guo and Leu, 2013). Additive manufacturing also known as additive fabrication, direct digital manufacturing and layer manufacturing. Figure 2.2 below illustrates one of the additive manufacturing process – Fused Deposition Modeling (FDM). Additive manufacturing is the first computer automated methods that able to produce physical model layer by layer according to 3D modeling in computer-aided design (CAD) using various kind of materials, such as metal, ceramic, plastic, and composite material (Huang et al., 2015).

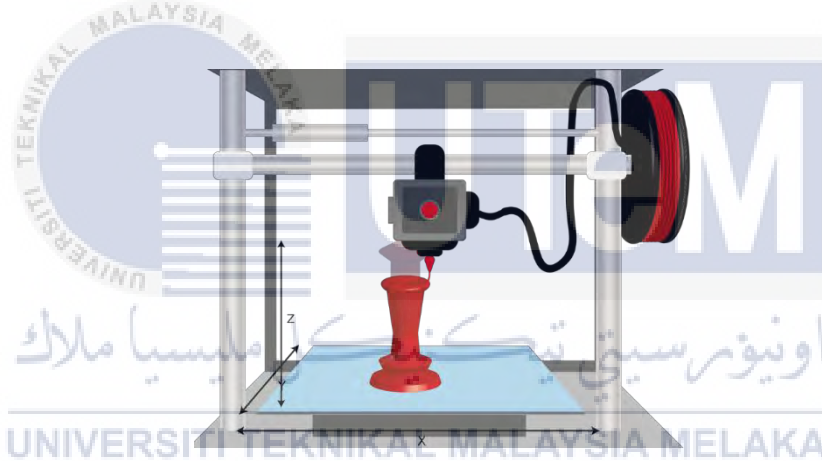


Figure 2.2: Fused Deposition Modeling Process (Raghavan, K., 2016).

One of the advantages of additive manufacturing is the ability to fabricate complex model rapidly without the use of additional fixtures and cutting tools (Huang et al., 2013). Unlike subtractive manufacturing process, additive manufacturing able to construct complex geometries as shown in Figure 2.3 and consolidate all the separate parts into a single model. However, the curved surface or overhang geometry required additional support material while fabricating. The support material which is able to remove easily after the fabrication process. Besides that, design optimization and testing can be performed at the same time in

order to test product's functionality and marketability, hence, reducing the need for natural resource during the process.



Figure 2.3: Complex Air Duct System Used in Aerospace Industry Fabricate by Additive Manufacturing Process.

Furthermore, the flexibility of additive manufacturing allows manufacturers to optimize the product development lead time and further reduce the manufacturing cost with less human interaction (Gardan, 2015). According to Babu & Goodridge (2015) showed that additive manufacturing able to improve sustainability through the efficient use of the material. Figure 2.4 below illustrates the comparison waste of material between additive manufacturing and subtractive manufacturing. Unlike subtractive manufacturing using material removal techniques such as machining, punching and stamping to fabricate the product, additive manufacturing fabricates the product by depositing material layer by layer repeatedly until the final shape is formed.

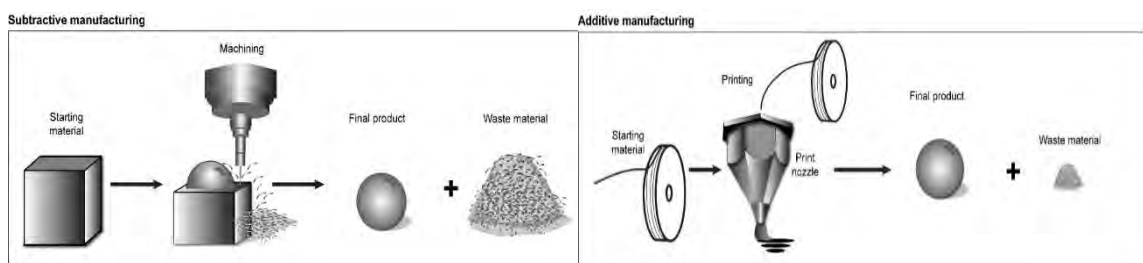


Figure 2.4: Conceptual Comparison between Subtractive and Additive Manufacturing.

2.1.2 Subtractive Manufacturing

According to Nafis et al. (2012), rapid prototyping can be classified into three categories, which is additive manufacturing, subtractive manufacturing and formative manufacturing. Subtractive manufacturing can be defined as “three dimensional (3D) object is produced by successively removing material from the workpiece that is bigger size than the final product” (M Nafis et al., 2012). In other hands, subtractive manufacturing also known as material removal process. Computer Numerical Control (CNC) machines such as CNC milling machine and CNC lathe machine are examples of subtractive manufacturing. CNC machine makes use of Computer Aided Manufacturing (CAM) software to control the cutting tool and with the help of fixture to clamp the model in position, the cutting tool removes material layer by layer until the final product is completed (Zahid, Case, and Watts, 2014). Figure 2.5 below demonstrates one of the subtractive manufacturing process – milling.

Advantages of subtractive manufacturing in term of material workability, unlike additive manufacturing usually restricted to several materials such as thermoplastics and resin. CNC machine offers a wide range of materials such as metal alloys, woods, acrylics, thermoplastics, aluminum, steel, brass, copper, etc. The selection of the cutting tool is depending on the hardness of the material. In term of mechanical properties, subtractive manufacturing able to produce the product with higher strength and robustness due to its ability to fabricate various kind of material with high Young’s Modulus value.

In term of precision, subtractive manufacturing such as CNC milling able to produce very high accuracy product. In contrast, staircase effect which commonly happened in additive manufacturing will greatly reduce the accuracy of the printed part. Although post-process method such as machining able to reduce the staircase effect, 3D printed part will tend to deform and further damage the part when exposed to high temperature (Pandey, Reddy, and Dhande, 2003).



Figure 2.5: Subtractive Manufacturing – Milling process.

2.2 Classification of Additive Manufacturing

According to Kruth (1991), material addition process can be classified according to the material state before part formation and the way of formation shape is built. Figure 2.6 below shows the classification according to the raw material state before part formation. Solid state raw material can further be classified into bonding thin sheets by using adhesive and bonding semi polymerized plastic sheets by photopolymerization. Liquid state raw material can further be categorized into liquid based material solidified by impact of light or laser and melting the material, depositing to form a layer and re-solidification of material. Powder state raw material also can be divided into melting the interfacial powder contact area and gluing the powder together by selectively adding a binder.

Another classification of material addition process is depending on the formation of shape is building. Figure 2.7 below shows the classification according to shape building technique, which are direct 3D technique and 2D layer technique.

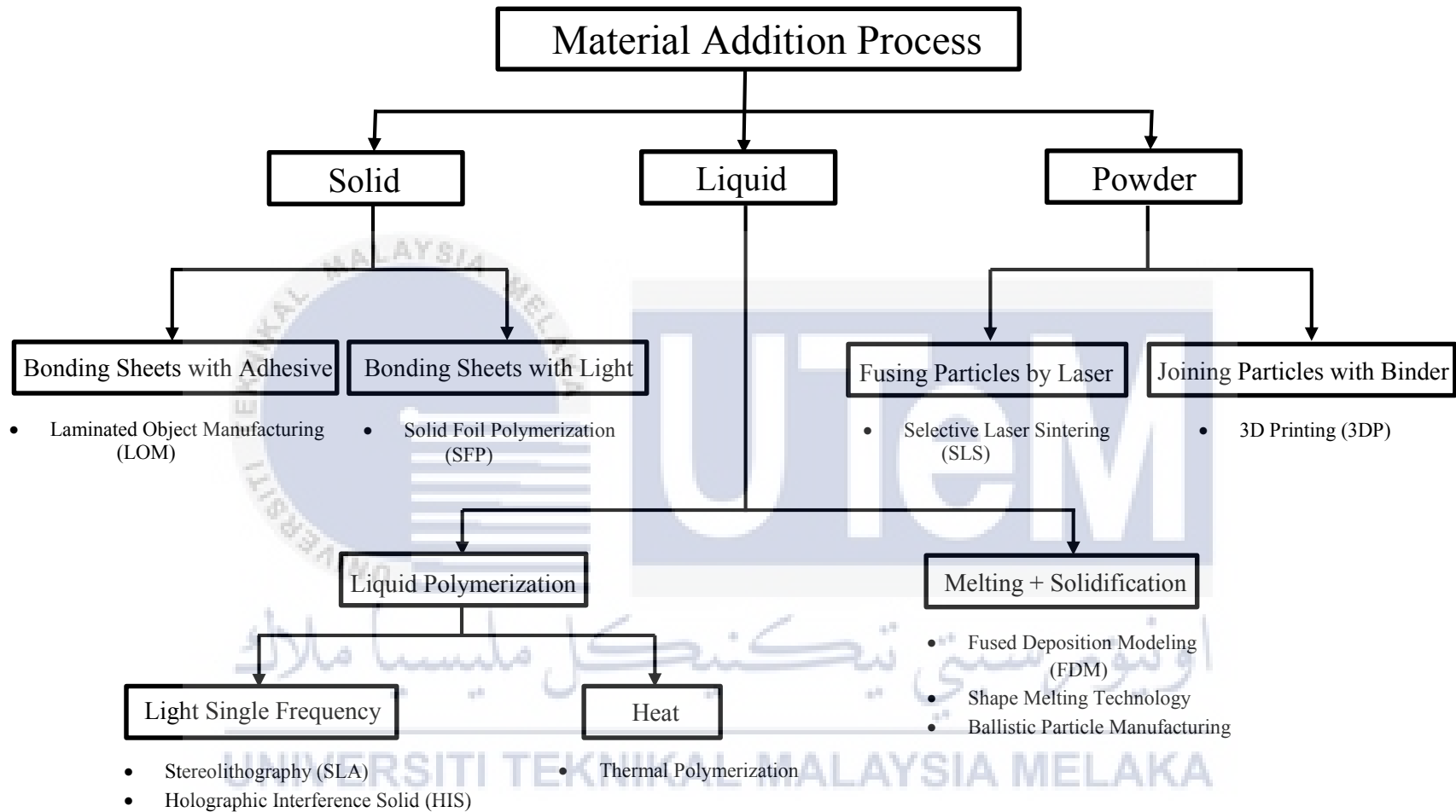


Figure 2.6: Classification of Processes According to Material State Technique (Kruth, 1991).

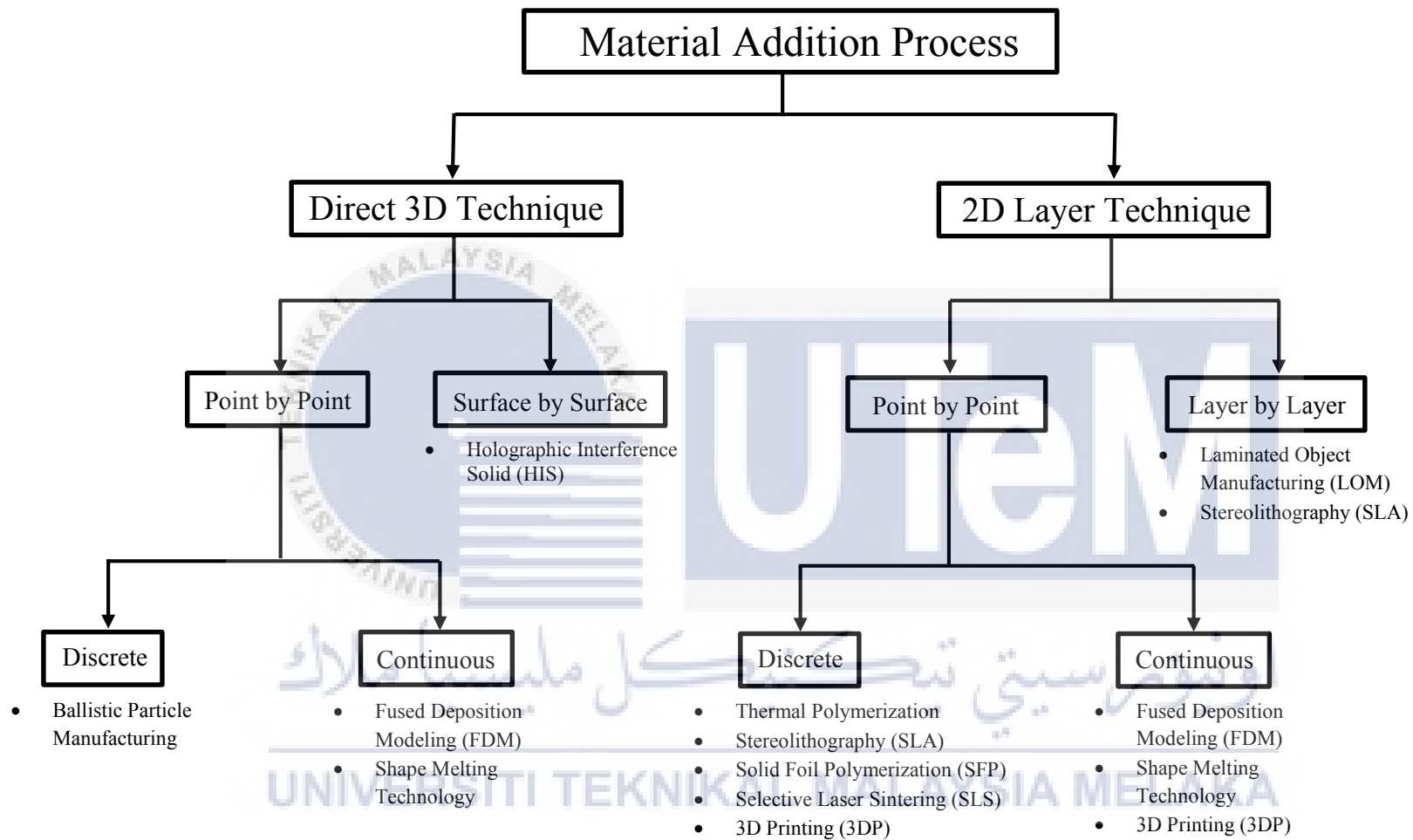


Figure 2.7: Classification of Processes According to Shape Building Technique (Kruth, 1991).

2.3 Fused Deposition Modeling (FDM)

Fused Deposition Modeling (FDM) process is one of the additive manufacturing technique for rapid prototyping. FDM is also known as Fused Filament Fabrication (FFF) (Gardan, 2015). FDM is classified as liquid-based rapid prototyping according to Kruth's first classification based on material creation technique (Kruth, 1991). FDM originally introduced by S. Scott Crump, founder of Stratasys in early 1992 (Boschetto and Bottini, 2014). The main concept of FDM is fabricating the model layer by layer from bottom surface until the top surface by depositing the melted thermoplastic filament (Bakar, Alkahari, and Boejang, 2010). Figure 2.8 below illustrates the concept of FDM.

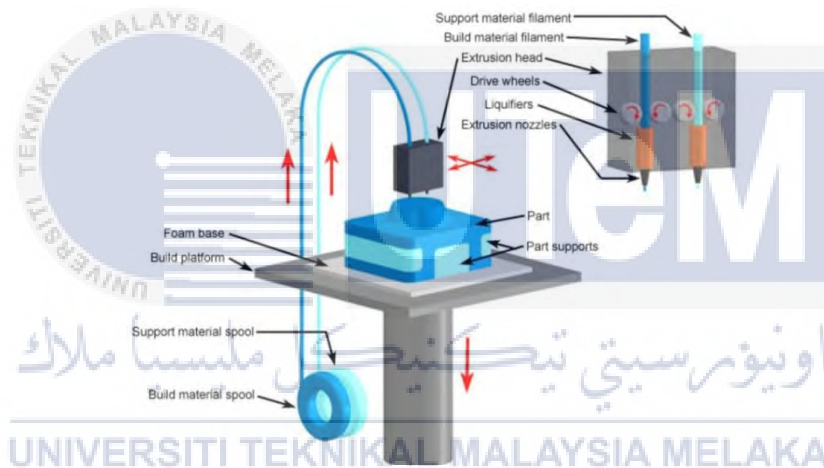


Figure 2.8: Fused Deposition Modeling (Graff, 2016).

2.3.1 Open Source Fused Deposition Modeling (FDM)

According to Free Software Foundation (2008), the term open source can be defined as “the license can be freely copied, redistribute and/or modify the hardware and software documentation and source code per the license requirement (Johnson et al., 2014). Open source software can be defined as software that can be freely accessed, source code modified and shared by anyone (Anonymous, n.d.). Open source hardware can be defined as a hardware that allows public to study, modify distribute, reproduce, sell the hardware based

on that design (Open Source Hardware Association, 2017). In other words, it means user can freely download the software and make modification in order to improve the design according to the specific user needs.

3D printer can be classified into high-end 3D printer, mid-end 3D printer, and low-end 3D printer. RepRap project is classified under the low-end 3D printer. RepRap project is an open source 3D printer which allows user to freely download the software and make modification on hardware according to user needs. RepRap project is known as replicating rapid prototyping (Sells et al., 2009). RepRap project able to self-replicate most of its own part and produce another 3D printer (Wittbrodt et al., 2013).

The RepRap project was started by Adrian Bowyer, a senior lecturer in University of Bath, England in 2005 (RepRap.org, 2017). Figure 2.9 below shows the first RepRap project known as Darwin 3D printer was produced in 2007.



Figure 2.9: First RepRap Project – Darwin (RepRap.org, 2017).

2.3.2 Working Principle of Fused Deposition Modeling (FDM)

In the FDM process, the thermoplastic filament is inserted into the extruder. The extruder is preheated to the filament 1° above the liquid melting temperature (Yan and Gu, 1996). The molten filament is then extruded through the nozzle onto the platform according to the movement controlled by the computer based on the designed part in 3D modeling. The platform is moved in Z-direction depends on the layer thickness parameter set in Repetier software. Figure 2.10 illustrates the FDM working principle.

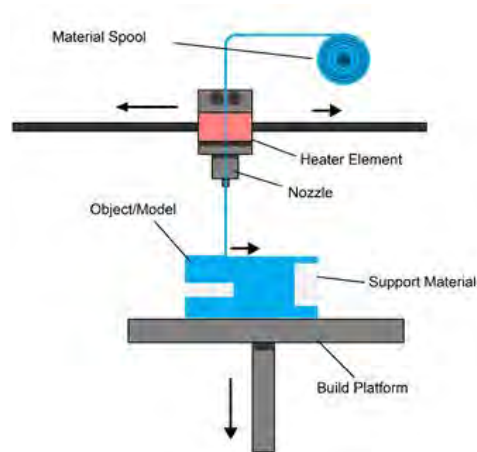


Figure 2.10: FDM Working Principle (MKS Technologies, 2016).

2.3.3 Advantages of Fused Deposition Modeling (FDM)

The main advantage of an open source FDM printing technology is sharing platform. Users are able to share their design around the world through the website such as Thingiverse, Youmagine and Grabcad. Another advantage of using open source FDM printer is cost saving. FDM printing technologies are widely used in Japan since long time ago but are considered as emerging technologies in Malaysia. As the technology is growing fast, the older version of the FDM printers are becoming obsolete. Many parts in the FDM printer are malfunctioning as the time past, such as part failure, reduced accuracy and precision. For the commercial FDM printer, maintenance is needed but is time-consuming to customize the failure part and the cost is very expensive. On the contrary, for the open source FDM printer, the failure part can simply be replaced by downloading the failure part 3D modeling file from the internet and replicate it using another FDM printer.

Besides that, open source FDM printing able to reduce technology cost in agriculture. It has potential to help the rural area communities. Farming equipment such as hand tools, food processing, animal management, water management, and hydroponics, as shown in Figure 2.11 can be easily printed using FDM printer. With the help of open source FDM printer, rural area communities are affordable and able to produce the farming equipment

effectively by downloading the cad file for free from open source file sharing platform, print it using a low-cost FDM printer. Hence, it saves a lot in term of cost. In conclusion, open source is an ethical and knowledge sharing concept, hence is the smart way to fight obsolescence and reduce living cost.

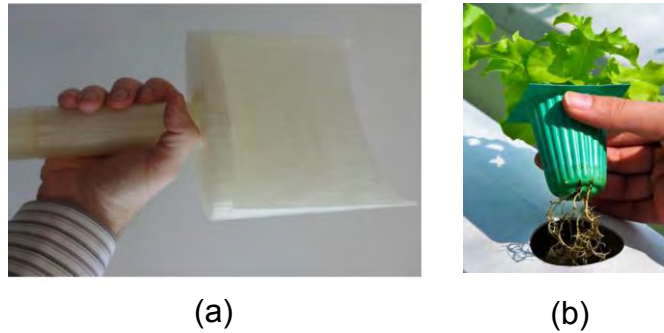


Figure 2.11: Farming Equipment, (a) Hand Shovel, (b) Hydroponics

2.3.4 Disadvantages of Fused Deposition Modeling (FDM)

FDM technology has the potential to infringe intellectual property right. With the help of the reverse 3D scanning technology, people can simply replicate the product which has copyright and trademarked into CAD file and share it virally. Due to that, the government is hard to control and protect the trademarked product.

Next disadvantage is product liability issue. This is a significant treat confronted by manufacturers and designers. For example, who shall be responsible for an open source FDM printed part which had cause malfunction in a machine? The designer who design the piping system or the manufacturer who download and print it using the 3D printer? There is also the issue of printing illegal item such as 3D printed gun which gone virally during the past few years in the United State of America.

2.3.5 Printing Material for Fused Deposition Modeling (FDM)

Thermoplastic materials, such as acrylonitrile butadiene styrene (ABS) and polylactic acid (PLA) are the most common and widely used material for FDM printer.

2.3.5.1 Acrylonitrile Butadiene Styrene (ABS)

ABS is undergone by the polymerization process of monomers, namely, acrylonitrile, butadiene, and styrene. ABS material is classified as oil-based thermoplastic, which is commonly used in the piping system, automotive sector and toy industry (Sean, 2017). Studies show that ABS is a biologically inert solid and considered non-toxic. ABS will not decompose in the landfill or aquatic system. ABS printed part offers good thermal stability, high chemical resistance, higher durability, flexibility and strength compared to PLA material (Olivera et al., 2016).

Acetone is a great solvent for many types of plastics. By exposing acetone chemical with ABS material, ABS able to produce a smooth outer layer of the surface part by dissolving the rough surfaces and producing strong bonding between the layers (Rao et al., 2012). Therefore, acetone chemical is widely used for surface finishing for ABS material printed part in FDM process.

2.3.5.2 Polylactic Acid (PLA)

PLA material, chemical formula: $(C_3H_4O_2)_n$ is an environmental friendly thermoplastic, made from biodegradable material, such as corn starch and sugarcane. PLA is widely used in 3D printing industry due to its cheapness, lower melting temperature and biodegradable. Besides that, studies show that warping effect tends to occur for ABS material compare to PLA material during 3D printing process (Sean, 2017). PLA material should be stored in less than 60°C and avoid contacting with atmospheric moisture in order to maintain its quality.

2.4 Introduction on Blow Cold Vapor Smoothing Treatment

Previous studies had proven that acetone is very effective solvent to treat surface roughness in vapor smoothing technique (Galantucci, Lavecchia, and Percoco, 2009). The vapor smoothing treatment as shown in Figure 2.12 was conducted in an enclosed chamber where the solvent was heated to produce solvent vapor. Solvent vapor was dispersed and surrounded the 3D printed part. Hence, it allowed the chemical reaction to occur and smoothen the outer layer without weakening the inner part of the printed part (US 8123999 B2, 2003). However, the current vapor smoothing technique exposed the solvent to high temperature. Some solvent, such as acetone is highly flammable and which might cause an explosion.

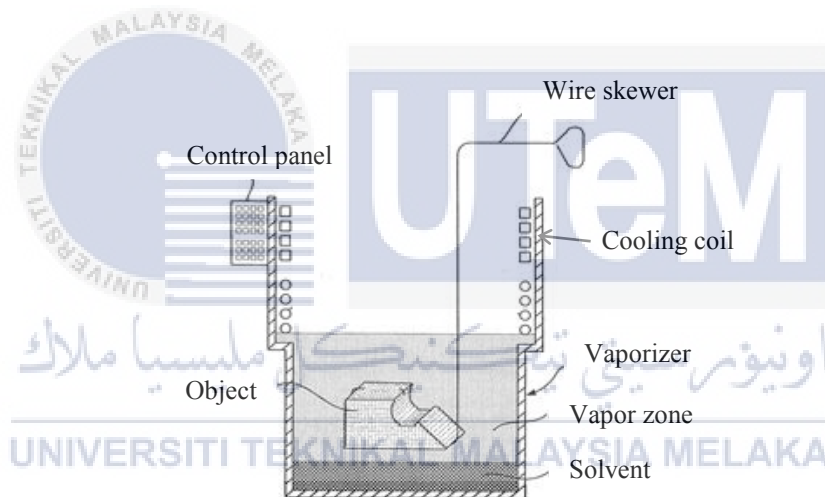


Figure 2.12: Vapor Smoothing Technique (Thomas, 2003).

By considering safety aspect, another vapor smoothing technique, known as Cold Vapor Smoothing treatment, which used acetone to improve the surface roughness of the FDM printed part was introduced. A wet paper towel dipped with acetone was used and allowed the paper towel to disperse the acetone vapor throughout the enclosed container (Garg, Bhattacharya, and Batish, 2016). This technique is effective but extremely time-consuming.

Another treatment was found to improve the surface roughness, namely acetone spraying technique. The concept of acetone spraying technique was pouring acetone into a spray can and the liquid acetone directly sprayed towards the printed part. This method is effective but produces inconsistent surface finishing (Michael, 2015).

All the previous studies had proved acetone as solvent agent is highly effective, economical to improve the surface finishing. A new vapor treatment technique, known as Blow Cold vapor treatment was introduced as shown in Figure 2.13. This technique does not involve heating process and able to produce consistent surface finishing throughout the part. The acetone solvent was being blown by a 12V fan to produce vapor acetone. The vapor acetone was then dispersed throughout the whole enclosed chamber and surrounded the printed part. Chemical reaction occurred between acetone vapor and the outer surface of printed part. In term of safety aspect, the treatment process was conducted in an enclosed chamber to prevent user from inhaling the vapor acetone which may cause harm towards the body, such as headache, dizziness, confusion, nausea, vomiting, etc.

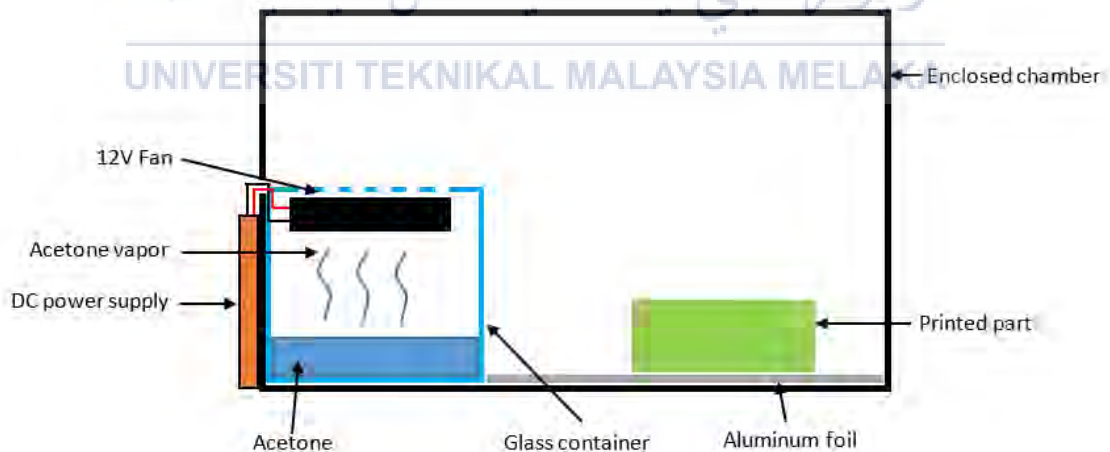


Figure 2.13: Blow Cold Vapor Smoothing Treatment

CHAPTER 3

METHODOLOGY

3.1 Introduction

In this research, optimum FDM printing parameters include infill density, layer height and temperature were investigated using Taguchi method in order to obtain the lowest surface roughness value. Next, the experiment was conducted using Bold Cold vapor treatment technique. Comparison between treated and untreated specimens was conducted in term of percentage of surface roughness and tensile strength affected. This chapter explains in details of this project.

3.2 Open Source FDM printer

In this project, open source FDM printer, namely Geeetech Prusa I3 was used. The specifications of the FDM printer used were listed in the Table 3.1 below. Figure 3.1 shows the Geeetech Prusa I3 FDM printer.

Table 3.1: FDM Printer Specification

Printer brand	Geeetech Prusa I3
Controlled board model	GT2560 Rev A+
Software	Malin I3 Pro C
No. of Nozzle	1 (Single)
Nozzle diameter	0.4mm
Filament diameter	1.75mm
Bed size	200mm x 200mm

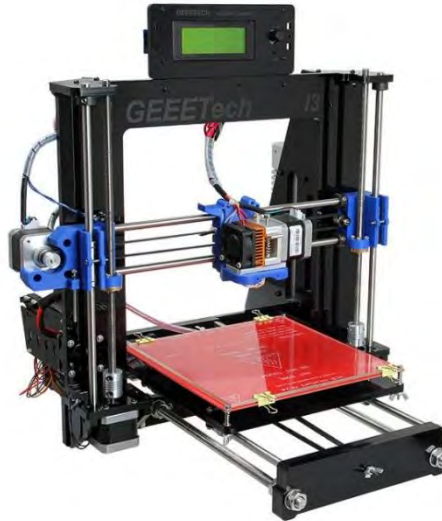


Figure 3.1: Geetech Prusa I3

3.3 Working Procedure of Fused Deposition Modeling (FDM)

FDM working procedure can be divided into pre-process, and post-process. Pre-process involves generating 3D modeling, slicing and converting into Standard Triangulation Language (STL) data and .gcode data. Post-process involves surface finishing process and improve mechanical properties.

3.3.1 FDM Pre-Process

3D modeling is defined as a process to generate 3D shaped object by manipulating the polygons and edges in the 3D generate platform (Justin, 2017). 3D modeling of the design part can be generated using Computer Aided Design (CAD) software, such as AutoCAD, Solidworks 3D, Catia, Fusion 360. 3D modeling also can be generated by using open-source CAD software, such as Blender, OpenSCAD and FreeCAD. Another method to generate 3D modeling data is through reverse scanning technologies by scanning the objects into a set of data points which represents the object digitally. Figure 3.2 below shows the 3D modeling file of the dogbone-shaped specimen is generated using Catia CAD software.

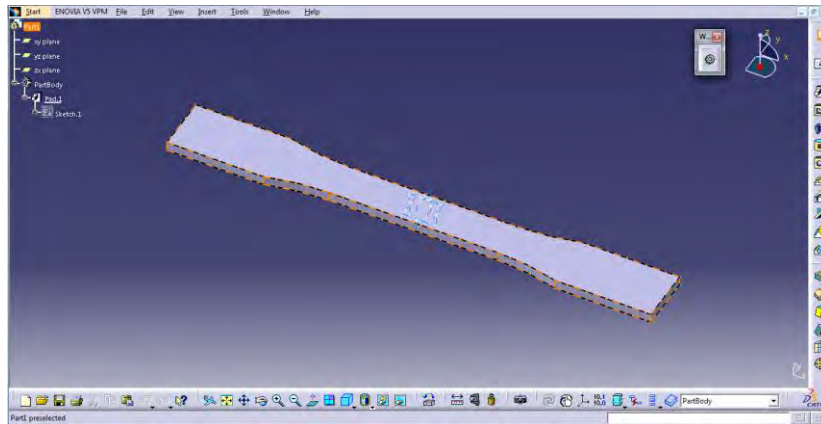


Figure 3.2: 3D Modeling Generated using Catia CAD Software

The designed part was saved in Standard Triangulation Language (STL) format. STL file is a format that used to store the information about 3D models. When integrates with 3D modeling slicing software such as open source Slic3r and Repetier software, it also allows communication between the computer and 3D printer (Dibya, 2017). The 3D printing parameters, such as infill density, layer height, infill angle, nozzle temperature, infill pattern and printing speed are required to operate the 3D printer. Figure 3.3 shows the 3D model is sliced according to the printing parameters using Repetier software.

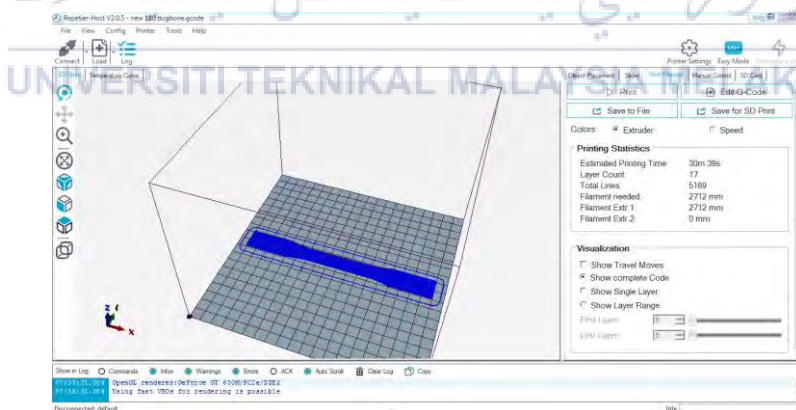


Figure 3.3: Repetier Software

The next step is converting the sliced 3D model into g-code format. G-code is a machine language and mainly used in industry to control the movement of the automated machine, for example, CNC machine (ThomasNet, 2017). The g-code file is loaded to 3D printer software, such as Pronterface software to allow communication with the 3D printer.

Pronterface software contains the information of the 3D printer and allows to control the movement of the nozzle head and its temperature. Figure 3.4 below shows the 3D model g-code file is uploaded to Pronterface software and ready to be printed.

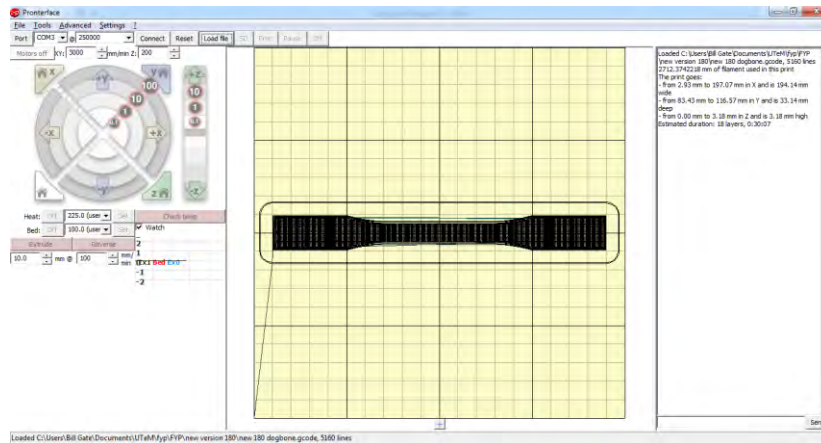


Figure 3.4: Pronterface Software

3.3.2 FDM Post-process

The main purpose of post-processing for FDM printed part is to improve the surface finishing and enhance the mechanical properties. There are several post-process methods to improve the mechanical properties of the printed product, such as sanding, cold welding, gap filling, polishing, painting, vapor smoothing, dipping, epoxy coating, and metal plating. Figure 3.5 below shows the different post-process methods: (a) cold welding, (b) gap filling, (c) unprocessed, (d) sanded, (e) polished, (f) painted, (g) epoxy coated.

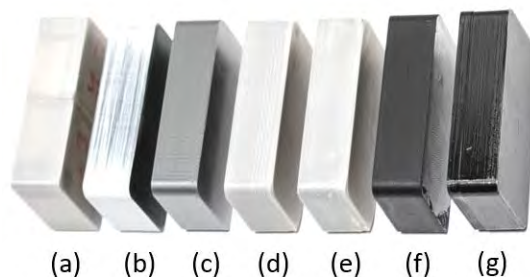


Figure 3.5: Different Post-Processing Methods (Enza3D, 2017).

In this study, vapor smoothing technique was used to improve the surface roughness of the specimen. Vapor smoothing utilized the chemical solvent to smoothen the outer surface of the specimen. This process reduced the layer lines formed on the surface of the printed part. With the optimum chemical solvent exposure time, this process able to preserve the feature detail and accuracy of the printed part. If uncontrollable amount of chemical solvent is used, overexposure condition is happened, which has a heavy impact on tolerances and strength of the printed part. Figure 3.6 below shows the comparison between vapor smoothing treated and untreated printed part. As shown in Figure 3.6(b), this process able to smoothen the surface of the printed part and provide a shiny surface around the exterior of printed part.

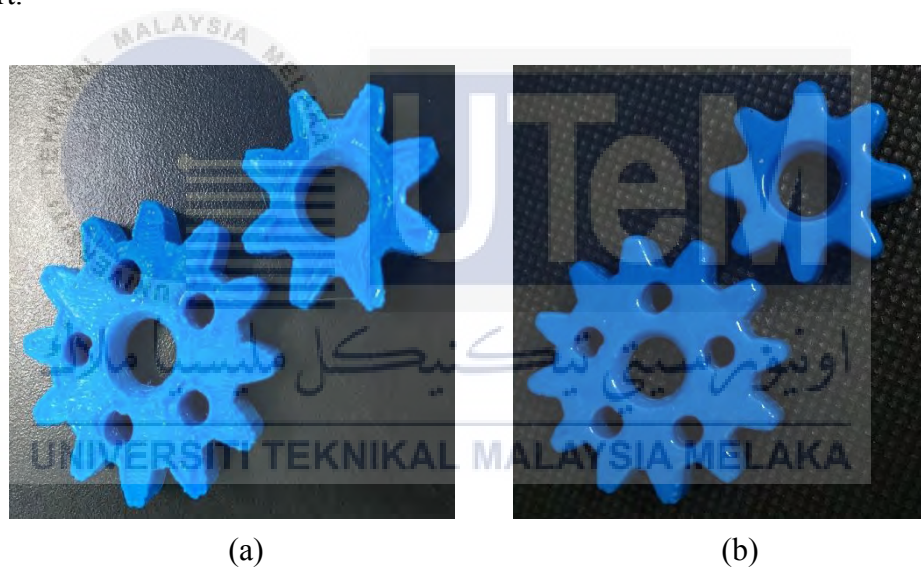


Figure 3.6: Vapor Smoothing (a) Before Treatment, (b) After Treatment

3.4 Project Specimen

In this project, dogbone-shaped specimen according to ASTM D638 Type I were printed based on the optimum printing parameters defined using Taguchi method. The specimens were printed using Geetech Prusa I3 3D printer with ABS as printing material. ASTM D638 Type I is commonly used to perform tensile strength test. The dimension of the dogbone-shaped specimen is shown in Figure 3.7 (ASTM International, 2004).

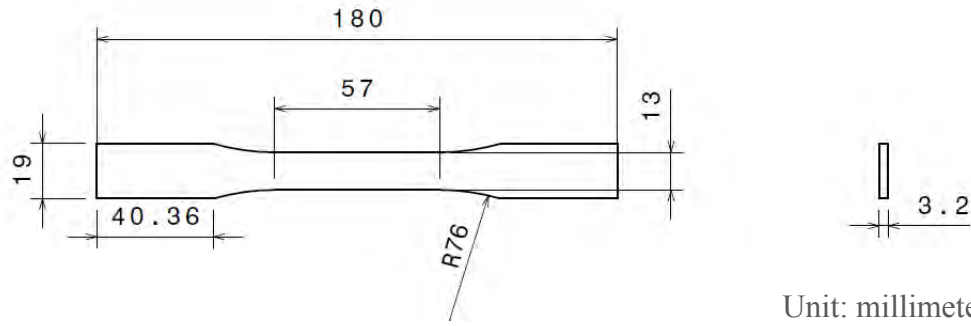


Figure 3.7: Dogbone-shaped Test Specimen

3.5 Apparatus

3.5.1 Shimadzu Ag10kNX Universal Testing Machine

In this project, Shimadzu Ag10kNX Universal Testing machine was used to determine the tensile strength of the printed part. The tensile strength test was conducted after printed part was being exposed to vapor acetone in Blow Cold vapor treatment process. The acetone vapor was allowed to fully vaporize for 24 hours before the tensile strength test was conducted. The experiment was conducted with velocity speed of 5 mm/min according to ASTM D638 standard. The results were compared between vapor treated part and untreated part. Figure 3.8 below shows the Shimadzu Ag10kNX universal testing machine used in this study.



Figure 3.8: Shimadzu Ag10kNX Universal Testing machine

3.5.2 Shodensha GR3400 3D Non-Contact Profilometer

Shodensha GR3400 3D Non-Contact Profilometer with 5x magnifying scope lens was used in this project to determine the surface roughness value of the specimens. 3 different spots on the surface of the specimen were measured and average surface roughness value was calculated. The unit of measurement was in micrometer (μm). Surface roughness comparison between acetone vapor treated and untreated specimen was conducted. Figure 3.9 below shows the Shodensha GR3400 3D Non-Contact Profilometer that used in this study.



Figure 3.9: Shodensha GR3400 3D Non-Contact Profilometer

3.5.3 Blow Cold Vapor Treatment Chamber

The specification of the Blow Cold vapor treatment chamber used in this project is listed as shown in Table 3.2 below.

Table 3.2: Specification of Blow Cold Vapor Treatment Chamber

Power Supply	12V, 0.18A
Dimension, mm	210 x 180 x 150
Material	Glass

3.5.4 Acetone

The specification of the acetone solvent used in this project is listed as shown in Table 3.3 below.

Table 3.3: Chemical Properties of Acetone

Chemical formula	(CH ₃) ₂ CO
Appearance	Liquid form, Colorless
Density, g/cm³	0.79
Acetone exposure time (min)	30 to 210

3.6 Location

This project was conducted in Technology Campus, University Technical Malaysia Melaka (UTeM). Table 3.4 below shows the location where the experiment was conducted.

Table 3.4: Experiment Location

Test	Location
Specimen printing	Innovation and Prototyping Research lab, FKM
Blow Cold vapor treatment	Chemistry lab, FKM
Tensile strength test	AMCHAL lab, Makmal Kejuruteraan Mekanikal
Surface roughness test	Tribology lab, FKM

3.7 Design of Experiment

Design of Experiment (DOE) is used to determine the relationship between the key parameters that affecting a process and the result value of the process (Sundararajan, 2000). Figure 3.10 below explained the relationship between factors that affecting a process and its output response. The controllable input factors are referring to the input data that can be adjusted the value in an experiment. Uncontrollable input factors refer to the factors that are unable to make modification on the parameter in an experiment. Responses mean the process outcome that determines the desired result of the experiment (Dean, 2017).

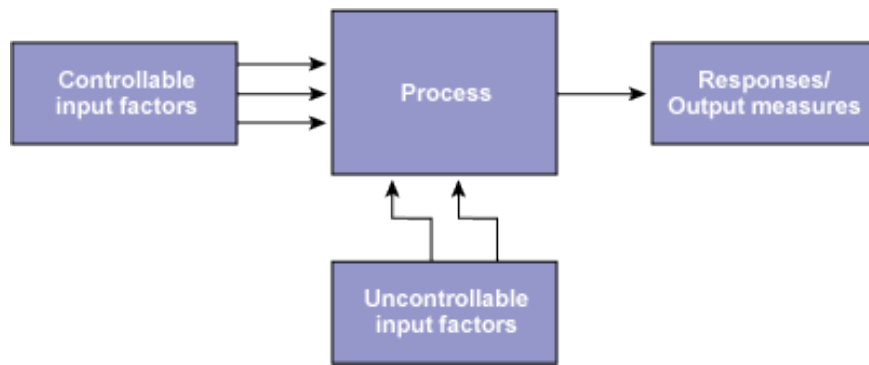


Figure 3.10: Process Factors and Response

3.7.1 Taguchi Method

Industrialization is considered as the symbolic of growth in the developing countries. It is always desirable to improve quality of the product and at the same time reduce costs, unwanted designs and processes associated with products and services in an industry. Variation in the desirable quality of the product is normally because of the settings prescribed in the controllable factors which values can be monitored and adjustable and uncontrollable factor where value can be measurable but difficult to adjust (Mitra, 2011). Taguchi method was introduced and developed by Genichi Taguchi and the main purpose is to investigate the key parameters that influencing the process performance and the parameters value to meet the target performance (Antony et al., 2001). Signal-to-noise (S/N) ratio is defined as the quality that can be quantified in term of the process response to the signal factors and noise factors (Statsoft, 2017). In order to improve the quality of the product, the best settings for the controllable factors need to be determined and the S/N ratio needs to be maximized.

There are three functional formulation of the S/N ratio, which is depending on the nature of the process characteristic. Equation (3.1) shows the S/N ratio for smaller-is-better process characteristic. Equation (3.2) shows the S/N ratio for nominal-is-better process characteristic, while Equation (3.3) shows the S/N ratio for larger-is-better process characteristic.

i) Smaller-is-better

Smaller-is-better can be used to minimize some unwanted product response.

$$SN_S = -10 \log \left(\frac{\sum_{i=1}^n y_i^n}{n} \right) \quad (3.1)$$

,where SN_S is referred to total resultant of the S/N ratio, n is number of observation made on the variable y_i and y is the variable characteristic.

ii) Nominal-is-better

Nominal-is-better can be used by setting the signal value with the desirable value, where ideal quality is equated to the desirable nominal value and base the S/N ratio on means and standard deviations. The formula to compute the nominal-is-better is:

$$SN_N = 10 \log \left(\frac{\bar{y}^2}{s^2} \right) \quad (3.2)$$

,where \bar{y} is the mean value for variable y and s^2 is the variance.

iii) Larger-is-better

Larger-is-better can be used to maximize the desirable product response value. The formula to compute the larger-is-better is:

$$SN_L = -10 \log \left(\frac{\sum_{i=1}^n 1/y_i^2}{n} \right) \quad (3.3)$$

,where n is number of observation made on the variable y_i and y is the variable characteristic.

Taguchi design advocates three stages design process methodology to determine the setting and tolerances for the controllable factors (Lupulescu, Yordanova, & Mladenov, 2011). The first stage of Taguchi design is known as system design. Creativity, innovation and related engineering experiences are involved to design the product characteristics,

features and technical parameters in order to meet the objectives of the product requirement. Controllable and uncontrollable factors are determined at this stage.

The second stage of Taguchi design methodology is parameter design. In this stage, an optimal parameter value of the controllable factors is determined either to minimize the response output, maximize the desirable product response value or achieve the target level in response. An appropriate S/N ratio formulation is chosen based on the objective of the product requirement to incorporate both the variation in the response value and its desired target value (Mitra, 2011).

The third stage of the Taguchi design is known as tolerance design. This stage is only applicable if the optimal parameter value obtained in stage two is not acceptable. This might be due to various factors, such as manufacturing cost, manufacturability, etc. The main purpose of tolerance design is to determine the acceptable range of variation between the controllable factors.

Taguchi orthogonal array is a highly fractional orthogonal design that depends on the design matrix which allows considering a selected subset of combinations of multiple factors at multiple levels (Yang and El-Haik, 2008). Taguchi orthogonal array can be evaluated independently due to all level of factors are arranged equally. By using the orthogonal array, the number of experiments needed to run can be minimized and at the same time retaining the pair-wise balancing property. Table 3.5 below shows an example of the Taguchi experimental design, using L9 array with three design factors, each at three levels. Total 27 experiments are needed to run in the full factorial experiment. In order to reduce the number of experiments need to run, Taguchi orthogonal array is used. The L9 refers to a total of 9 experiments need to run.

Table 3.5: Taguchi Orthogonal Array

Number of experiments	Factor 1	Factor 2	Factor 3
1	Level 1	Level 1	Level 1
2	Level 1	Level 2	Level 2
3	Level 1	Level 3	Level 3
4	Level 2	Level 1	Level 2
5	Level 2	Level 2	Level 3
6	Level 2	Level 3	Level 1
7	Level 3	Level 1	Level 3
8	Level 3	Level 2	Level 1
9	Level 3	Level 3	Level 2

The optimum parameters can be determined using Minitab® 18.1 version software. The three input factors that influenced the surface roughness of the printed part were identified, which were layer thickness, infill density and temperature. Three levels were included in each factor. The factor level was determined based on the manufacturability criteria for the Geetech Prusa I3 printer.

3.8 Flow Chart

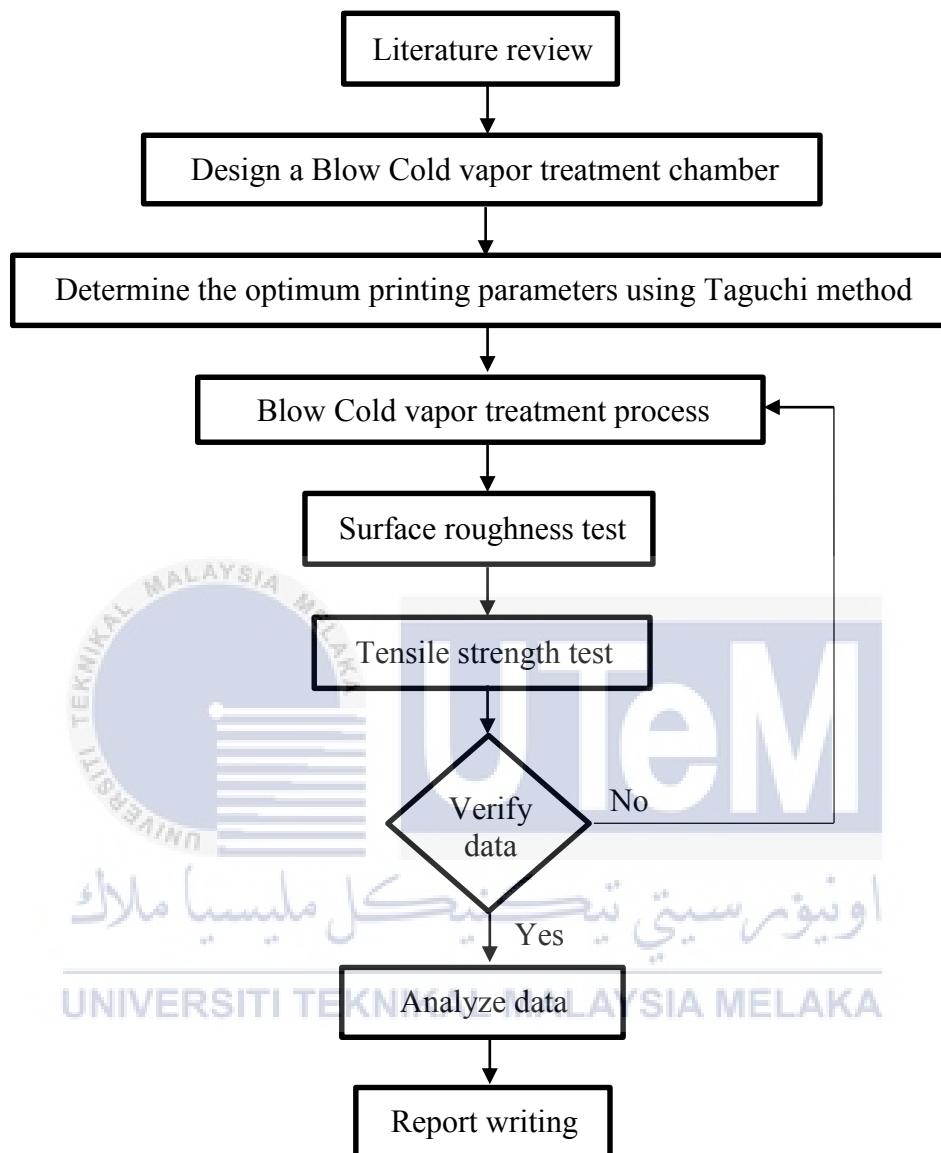


Figure 3.11: Flow Chart

CHAPTER 4

RESULTS AND ANALYSIS

4.1 Blow Cold Vapor Smoothing Treatment Container

Figure 4.1 below shows the blow cold vapor smoothing treatment container designed using Catia V5R20 software. The container dimension is 210mm (L) x 180mm (W) x 150mm (H). The top cover can be slide out in order to put in the specimens easily.

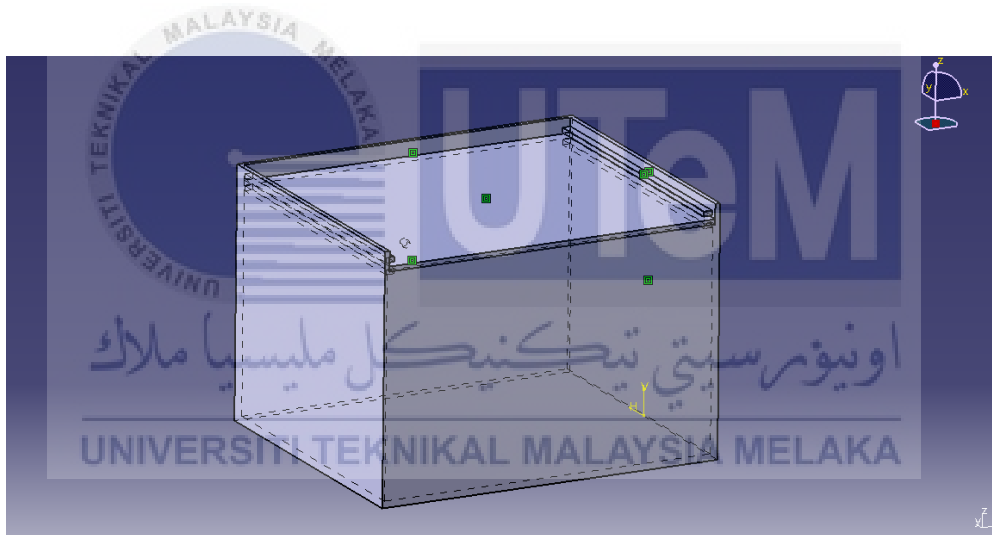


Figure 4.1: Blow Cold Vapor Smoothing Treatment Container

Figure 4.2 below shows the acetone container designed using Catia V5R20 software. The main purpose of the acetone container was to hold the acetone and a fan was attached on top of it to blow towards at acetone and allowed acetone vaporization occurred. The dimension of the acetone container is 100mm x 100mm x 100mm.

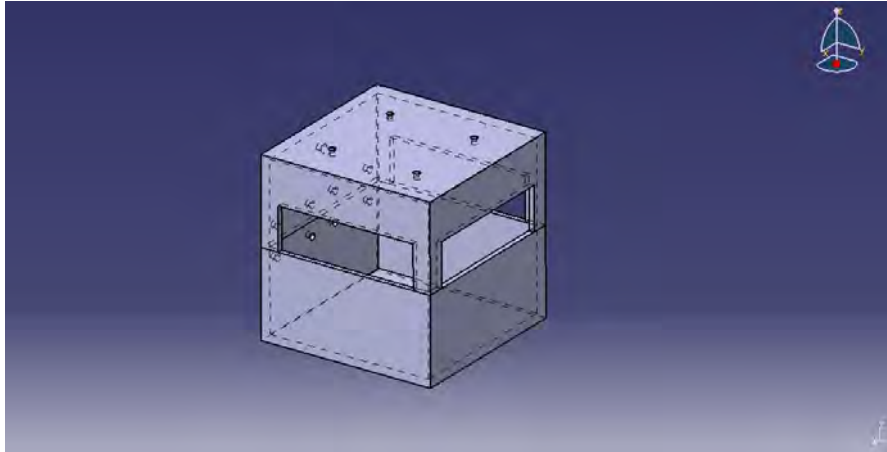


Figure 4.2: Acetone Container

The Blow Cold vapor smoothing treatment container was fabricated using glass material, while the acetone container was fabricated using aluminum material. Table 4.1 and 4.2 below are the specifications for both of the containers.

Table 4.1: Blow Cold Vapor Smoothing Treatment Container Specification

Dimension, (mm)	210 (L) x 180 (w) x 150 (h)
Material	Glass
Thickness (mm)	5

Table 4.2: Acetone Container Specification

Dimension, (mm)	100 (L) x 100 (w) x 100 (h)
Material	Aluminum
Thickness (mm)	0.5

Due to the chemical properties of acetone is being served as the chemical solvent, experiment must be conducted to determine which sealant is the best to joint between the plates and able to resist the acetone corrosion. Four different type of sealants were being tested in this experiment. The ability to resist acetone corrosion can be tested by applying 5N force at the end of the plates. Figure 4.3 demonstrates the schematic diagram of the experiment to test the resistibility of sealants towards acetone corrosion.

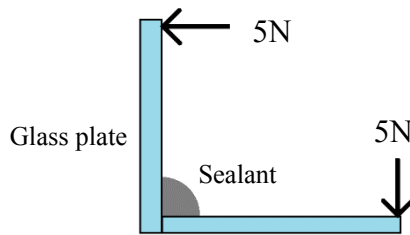


Figure 4.3: Acetone Corrosion Resistibility Experiment

Table 4.3 below shows the comparison between four different type of sealants, its required curing time and its ability to resist acetone corrosion. Hardex Clear Silicone Sealant is 100% silicone rubber and must be cured for 16 hours. V-tech UV Super Glue has the properties of low viscosity, fast curing time and Ethyl based Super Glue which joint immediately upon contact between objects. Araldite Epoxy Adhesive requires the mixture of resin and hardener with the ratio of 1:1 and the required curing time at least 24 hours in order to produce strong bond between objects. X'Traseal Room-Temperature-Vulcanizing (RTV) Silicone Sealant is the mixture of Oxime (neutral cure) and silicone rubber with the required curing time of 16 hours. Methyl Ethyl Ketone (MEK) and Toluene is acted as the solvent for RTV glue, but no reaction towards acetone corrosion.

Table 4.3: Comparison between 4 Different Sealants and Its Ability to Resist Corrosion.

Sealants	Hardex Clear Silicone Sealant	V-tech UV Super Glue	Araldite Epoxy Adhesive	X'Traseal RTV Silicone Sealant
Description				
Required Curing time	16 hours	2 hours	24 hours	16 hours
Ability to resist acetone corrosion	Unable to resist	Unable to resist	Unable to resist	Able to resist but silicone was soften

Figure 4.4 and 4.5 below show the complete fabricated Blow Cold vapor smoothing treatment container and acetone storing container. X'Traseal RTV Silicone Sealant was chose as the sealant to join the plates.

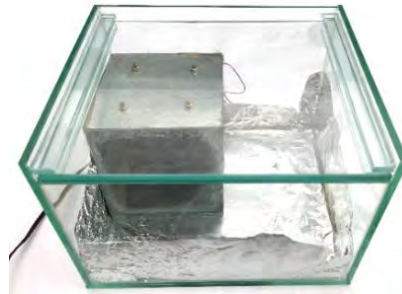


Figure 4.4: Blow Cold Vapor Smoothing Treatment Container

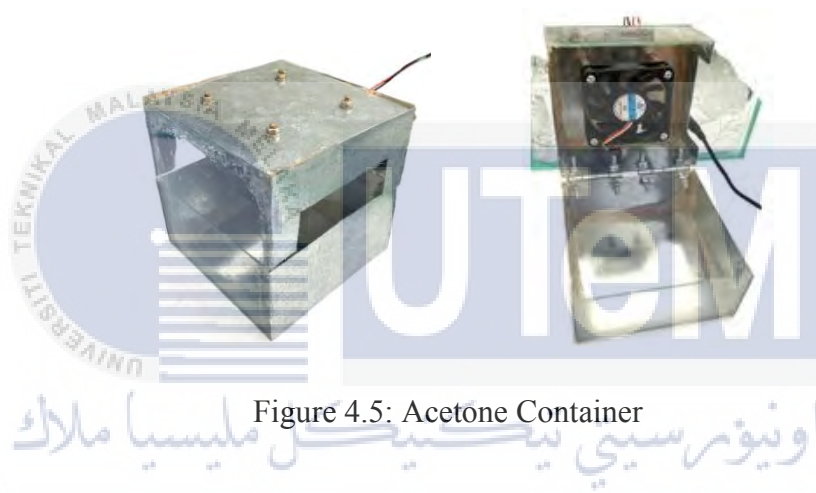


Figure 4.5: Acetone Container

4.2 Process Parameters

The experiment was conducted by using low cost 3D printer – Geeetech Prusa I3. There were several process parameters such as nozzle temperature, infill density, layer thickness, and build up orientation are critical factors that affect the mechanical properties of the printed part. Previous research done by Mazlan (2018) about the effect of three important parameters such as layer thickness, infill density and raster angle on surface roughness of the 3D printed part. The result shows that raster angle has no significant effect on the surface roughness of the 3D printed part. In this study, effect of process parameters such as layer thickness, infill density and temperature on surface roughness of the 3D printed part were being investigated. The printing parameters are briefly defined as follows:

- (a) *Layer thickness*: The measure of thickness of each successive layer deposited by nozzle in 3D printing process.
- (b) *Infill density*: The amount of plastics are printed inside the part.
- (c) *Temperature*: The nozzle temperature during printing process.

Various process parameters were held constant throughout the experiment at the value as tabulated in Table 4.4 below.

Table 4.4: Fixed Parameters throughout the Experiment

Parameters	Description
Nozzle diameter	0.4 mm
Bed temperature	100 °C
Infill pattern	Line
Raster angle	0° / 90°

The specimens were printed according to the ASTM D638 Type I standard with the printing parameter combinations calculated by using Taguchi method. Taguchi method was done using Minitab 18.1 version software with three factors and three levels (3^3) with an orthogonal array of L9, which required a total of nine experiments to be run. The printing parameters and its level are tabulated in Table 4.5 below.

Table 4.5: Printing Parameters and Its Level

Printing parameters	Unit	Level		
		1	2	3
Layer thickness	mm	0.18	0.22	0.25
Infill density	%	30	60	90
Temperature	°C	210	225	240

4.3 Surface Roughness

The surface roughness of the printed part was measured using 3D non-contact surface profilometer. To ensure data accuracy and consistency, three readings were taken at different spots on the 3D printed part as shown in Figure 4.6, which are 30mm, 90mm and 150mm from the origin.

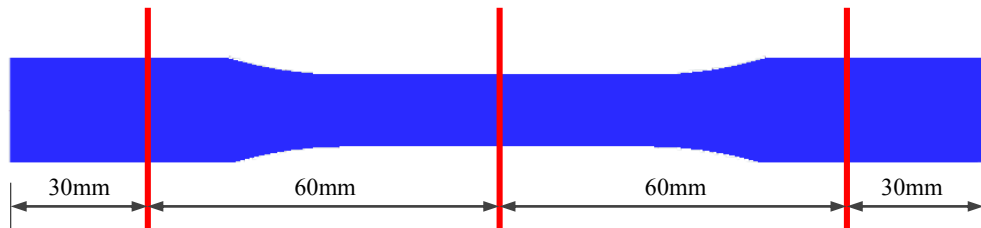


Figure 4.6: Surface Roughness Measuring Spots


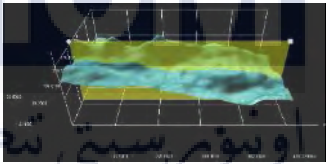

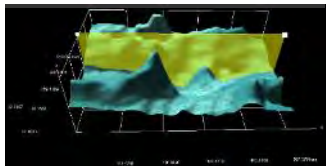

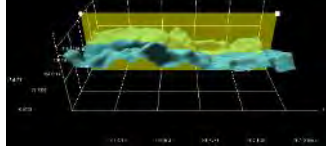

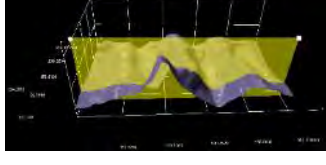
The experiment was repeated two times in order to achieve the accurate and consistent surface roughness value. The measured surface roughness value on the printed surface was tabulated in Table 4.6 below.

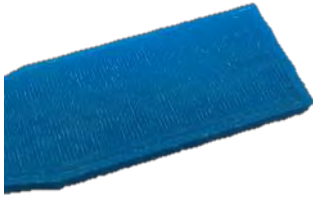
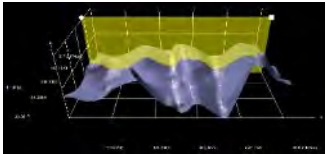

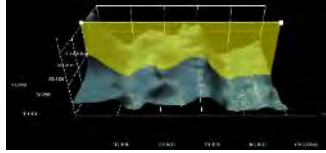

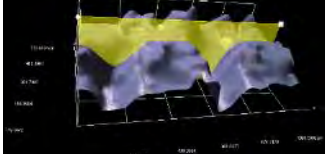

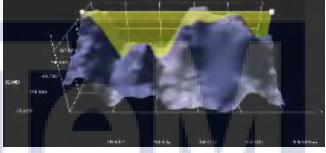

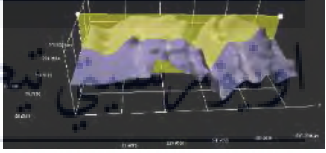
Table 4.6: Experimental Result for Surface Roughness Value at Three Different Spots

No.	Process parameters			Surface roughness, Ra (μm)						
	Layer thickness, mm	Infill density, %	Temperature, $^{\circ}\text{C}$	30mm		90mm		150mm		Average
				1	2	1	2	1	2	
1	0.18	30	210	2.22	3.71	6.82	2.01	4.97	2.89	3.77
2	0.18	60	225	4.09	2.72	2.89	1.56	6.36	2.64	3.37
3	0.18	90	240	2.85	2.59	2.68	6.06	3.06	2.58	3.30
4	0.22	30	225	13.75	11.55	13.83	12.13	11.26	12.03	12.43
5	0.22	60	240	6.63	8.49	9.72	20.28	8.03	15.83	11.50
6	0.22	90	210	18.49	19.05	8.78	5.49	13.33	11.01	12.69
7	0.25	30	240	16.03	19.57	19.07	19.60	15.02	19.87	18.20
8	0.25	60	210	14.38	13.60	13.69	12.82	13.85	13.49	13.64
9	0.25	90	225	19.14	12.45	14.53	15.68	11.14	16.67	14.94

Results indicated that the highest surface roughness value obtained when layer thickness was 0.25mm, infill density was 30% and temperature was 240°C, which the surface roughness value obtained was 18.1968 μ m. The lowest surface roughness value obtained was 3.3052, when layer thickness was 0.18mm, infill density was 90% and temperature was 240°C. Table 4.7 shows the surface profile of the 3D printed part according to the process parameters and its corresponding surface roughness value.

Table 4.7: Physical Appearance and Surface Profile of the 3D Printed Part

No.	Process parameters			Physical appearance	Surface Profile	Average surface roughness value, Ra (μ m)
	Layer thickness, mm	Infill density, %	Temperature, °C			
1	0.18	30	210			3.7703
2	0.18	60	225			3.3756
3	0.18	90	240			3.3052
4	0.22	30	225			12.4262

5	0.22	60	240			11.4968
6	0.22	90	210			12.6940
7	0.25	30	240			18.1968
8	0.25	60	210			13.6405
9	0.25	90	225			14.9366

Based on the observation from physical appearance on the surface of the 3D printed part, inconsistent flow tended to occur when temperature was 210°C. Table 7 above shows when layer thickness was 0.18mm, infill density was 30% and temperature was 210°C, the inconsistent flow effect was clearly showed on the surface of the 3D printed part. This results in slightly increasing the surface roughness value. When the temperature increased to 240°C, small amount of bubbles effect and burn marks were observed on the surface of the 3D printed part, which might lead to higher surface roughness value. Another observation noticed on the surface of the 3D printed part was rough surface tended to occur when layer thickness was 0.25mm.

There are three categories of performance analysis in Taguchi method, which are lower-the-better, nominal-the-better and higher-the-better. The lower-the-better process performance analysis was used in this study to determine the optimal surface roughness value in 3D printing process. Table 4.8 below shows the experimental results for surface roughness value, Ra and its corresponding signal-to-noise ratio value, S/N ratio.

Table 4.8: Experimental Result for Surface Roughness and S/N ratio

Experiment run	Process Parameters			Measured surface roughness, Ra (μm)	S/N ratio for surface roughness
	Layer thickness, mm	Infill density, %	Temperature, $^{\circ}\text{C}$		
1	0.18	30	210	3.7703	-11.5275
2	0.18	60	225	3.3756	-10.5670
3	0.18	90	240	3.3059	-10.3858
4	0.22	30	225	12.4262	-21.8868
5	0.22	60	240	11.4968	-21.2115
6	0.22	90	210	12.6940	-22.0720
7	0.25	30	240	18.1968	-25.1999
8	0.25	60	210	13.6405	-22.6966
9	0.25	90	225	14.9633	-23.4850

Figure 4.7 shows the main effect plot for mean function with respects to layer thickness, infill density and temperature parameters. Figure 4.8 shows the main effect plot for S/N ratios response to layer thickness, infill density and temperature parameters. Table 4.9 illustrates the S/N ratio values for the experiment by factor level. The results found that layer thickness was the main contributor towards surface roughness value, followed by infill density and temperature. Temperature had less significant effect on the surface roughness value in this study.

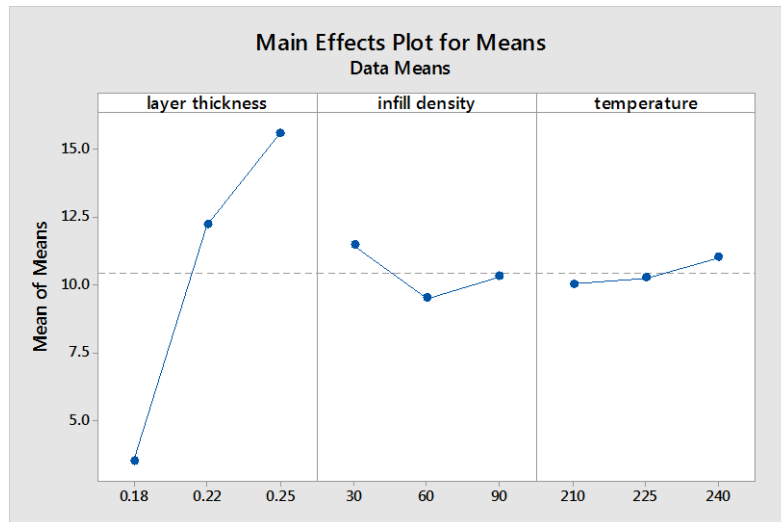


Figure 4.7: Main Effect Plot for Means

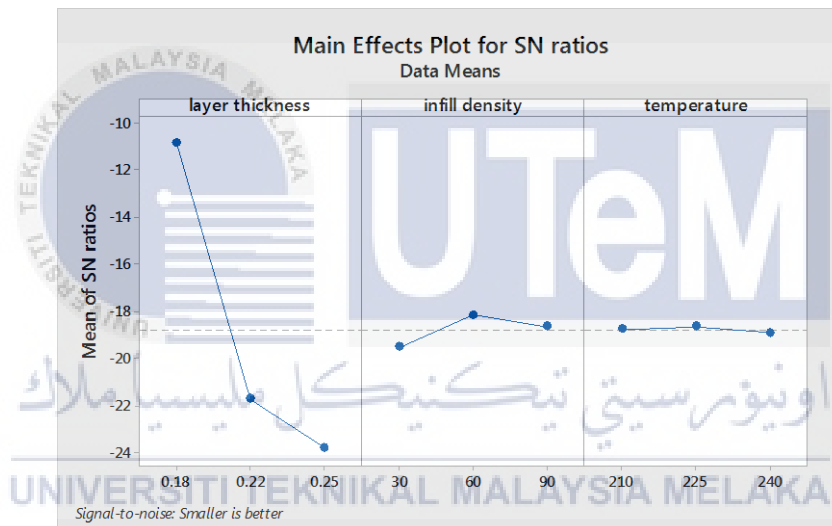


Figure 4.8: Main Effect Plot for S/N Ratio

Table 4.9: S/N Ratio Corresponding to Process Parameters and Its Level

Response Table for Signal to Noise Ratios (Smaller is better)			
Level	layer thickness	infill density	temperature
1	-10.83	-19.54	-18.77
2	-21.72	-18.16	-18.65
3	-23.79	-18.65	-18.93
Delta	12.97	1.38	0.29
Rank	1	2	3

Signal-to-noise ratio in Taguchi design is defined as the measure of robustness used to identify control factors that used to reduce variability in an experiment by minimizing the effect of uncontrollable factors (noise factors). Control factors is referring to the process factors that can be controlled, while noise factors cannot be controlled during a process. In a Taguchi designed experiment, noise factors can be manipulated to calculate the variability to occur and further identify the optimal control factor parameters which makes the process to have less effect on noise factors. Higher values of the signal-to-noise ratio (S/N) indicates that process parameters that has the minimum effects of the noise factors (Minitab, 2017). Based on Figure 8, highest S/N ratio occurs when layer thickness was 0.18mm, infill density was 60% and temperature was 225°C. Hence, the optimum printing parameters in this study which results in lowest surface roughness value obtained were layer thickness was 0.18mm, infill density was 60% and temperature was 225°C.

4.4 Blow Cold Vapor Smoothing Treatment

Dogbone specimens according to ASTM D638 standard were printed and left for 24 hours to allow plastic material completely solidified before the Blow Cold vapor smoothing treatment. From the previous research done by Mazlan (2018), the optimal acetone exposure time was three hours with 20 ml of acetone was being vaporized. The surface roughness value obtained was roughly 0.25 μ m. In this study, experiment had been conducted to examine the effect of volume of the container with respected to the volume of acetone needed to be vaporized. The previous research conducted the Blow Cold vapor smoothing treatment in a container with volume of 3610 cm³. The vapor smoothing treatment parameters that held constant in this experiment are tabularized in Table 4.10 below.

Table 4.10: Blow Cold Vapor Smoothing Parameter Conditions for 20 ml Acetone

Parameters	Description
Exposure time (min)	60 to 180
Solvent	Acetone
Volume (ml)	20

In this study, the Blow Cold vapor smoothing treatment container has the volume of 4250 cm³. Experiment was conducted with 20 ml of acetone to be vaporized. The surface roughness value was measured in three different spots, which were 30mm, 90mm, 150mm from the origin as shown in Figure 4.6. The measured surface roughness result was tabulated in Table 4.11. Figure 4.9 below shows the setting up equipment for the Blow Cold vapor smoothing treatment process.

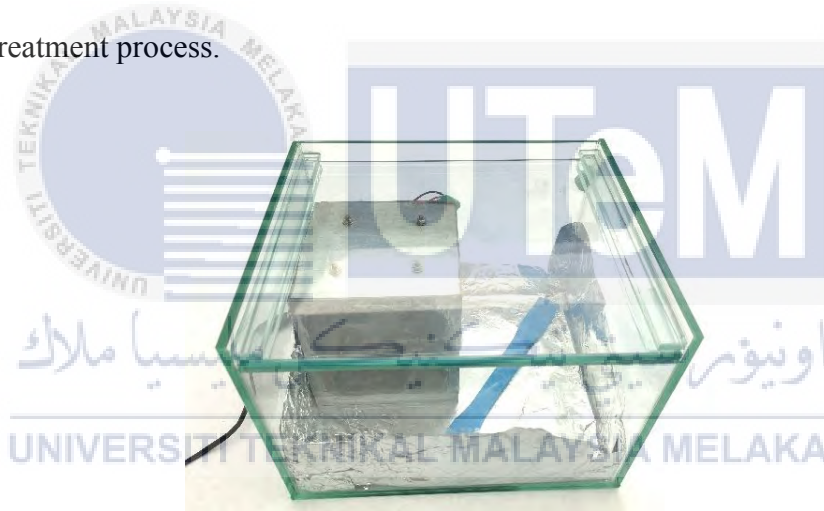


Figure 4.9: Blow Cold Vapor Smoothing Process

Table 4.11: Measured Surface Roughness Value against Exposure Time for 20 ml Acetone

No	Exposure time (minutes)	Surface roughness, Ra (μm)				Percentage of surface roughness reduced (%)
		30mm	90mm	150mm	Average	
1	0	4.0860	2.8873	6.3599	4.4444	0
2	60	2.4681	2.7978	2.1458	2.4706	44.41
3	120	1.2629	1.3850	1.2877	1.3119	70.48
4	150	0.4672	0.4827	0.3222	0.4241	90.46

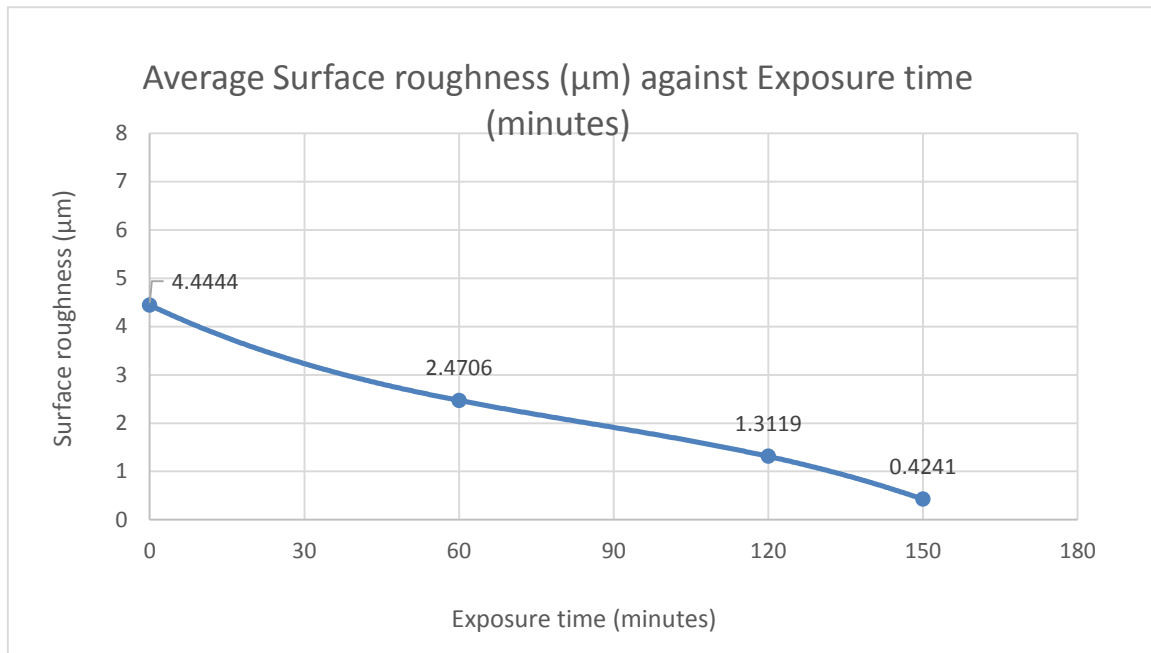

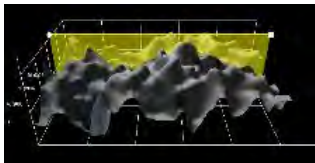

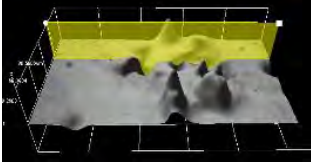

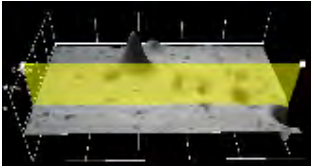


Figure 4.10: Graph of Average Surface Roughness against Exposure Time

It was observed that the 20 ml of acetone was completely vaporized in 150 minutes. The average surface roughness value obtained was $0.4241\mu\text{m}$. However, it was noticed that certain part on the surface of the specimen was not smoothen up especially near the edge of the specimen. This indicates that 20 ml of acetone was not enough in smoothening the surface of the specimen. Table 4.12 below are the surface profile of the specimens under Blow Cold vapor smoothening treatment with 20 ml of acetone.

Table 4.12: Surface Profile of the Specimens (20 ml Acetone)

No.	Exposure time (minutes)	Physical appearance	Surface Profile	Average surface roughness value, R_a (μm)
1	60			2.4706

2	120			1.3119
3	150			0.4241

In order to determine the optimal amount of acetone that needed to be vaporized in the new blow cold vapor smoothing treatment container with the volume of 4250 cm^3 , the ratio factor as shown in Table 4.13 below was used.

Table 4.13: Ratio Factor to Determine Amount of Acetone Needed

Volume of the container	3610 cm^3	4250 cm^3
Amount of acetone needed	20 ml	23.5 ml

The experiment was repeated using 23.5 ml of acetone to be vaporized and the surface roughness value was measured for every 30 minutes. Table 4.14 below shows the vapor smoothing treatment parameters which were held constant.

Table 4.14: Blow Cold Vapor Smoothing Parameter Conditions for 23.5 ml acetone

Parameters	Description
Exposure time (min)	30 to 210
Solvent	Acetone
Volume (ml)	23.5

The surface roughness values were measured in three different spots, which were 30mm, 90mm, 150mm from the origin as shown in Figure 4.6. The measured surface roughness result was tabulated in Table 4.15.

Table 4.15: Measured Surface Roughness against Exposure Time for 23.5 ml Acetone

No	Exposure time (minutes)	Surface roughness, Ra (μm)				Percentage of surface roughness reduced (%)
		30mm	90mm	150mm	Average	
1	0	4.0860	2.8873	6.3599	4.4444	0
2	30	4.4815	2.9467	3.3553	3.5945	19.12
3	60	3.3637	1.7716	3.3889	2.8414	36.07
4	90	1.8874	2.0873	2.2401	2.0716	53.39
5	120	0.8980	0.9640	1.4858	1.1159	74.89
6	150	0.7865	0.5980	0.5500	0.6448	85.49
7	180	0.2685	0.1062	0.2568	0.2105	95.26
8	210	0.1203	0.0582	0.1184	0.0990	97.77

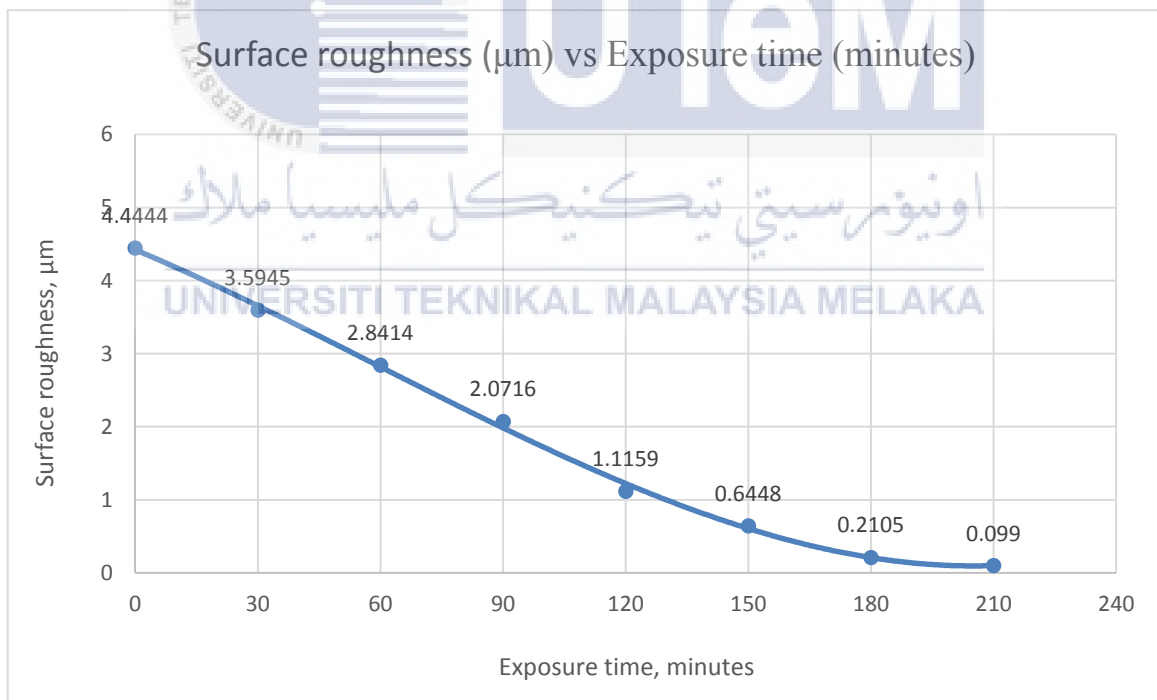


Figure 4.11: Graph of Surface Roughness against Exposure Time for 23.5 ml Acetone

As shown in the Figure 4.11, it was observed that the longer the acetone exposure time reacted on the surface of the specimens, the lower the surface roughness value. The acetone was completely vaporized after 210 minutes. The lowest surface roughness value obtained was $0.099\mu\text{m}$, which was 97.77% reduced when the acetone exposure time was 210 minutes. However, it was noticed that over-expose happened near the corner of the specimen during 210 minutes as shown in Figure 4.12. This results in reducing the specimen's accuracy.

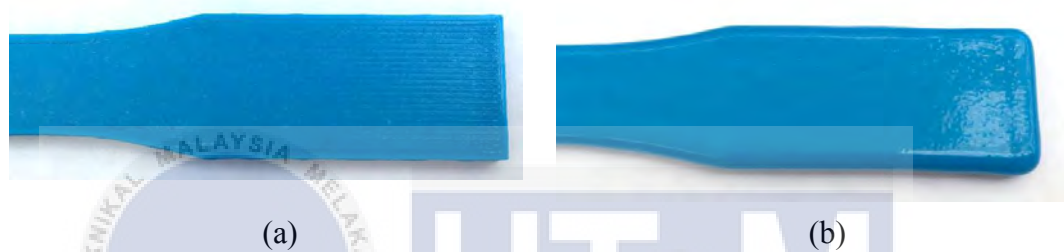


Figure 4.12: Dogbone Specimen (a) Before Treatment (b) After Treatment for 210 Minutes

Table 4.16 below were the surface profile of the specimens under Blow Cold vapor smoothing treatment with 23.5 ml acetone. The surface roughness value and surface profile of each specimens were measured for every 30 minutes interval. The optical image of the topmost surface of the specimens after blow cold vapor smoothing treatment were also taken using Shodensha microscope with 5x magnifying scope lens to observe the pattern line formed on the surface. The optical images were tabulated in Table 4.17.

Table 4.16: Surface Profile of the Specimens (23.5 ml Acetone)


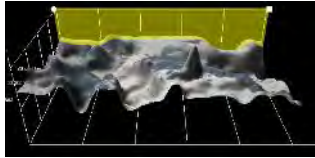

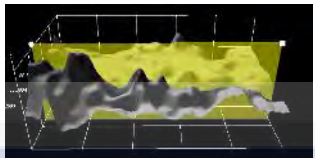

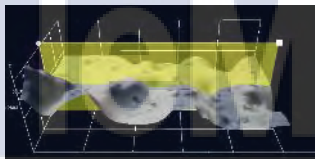



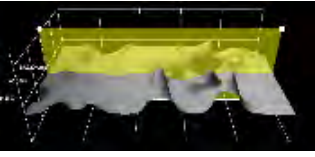

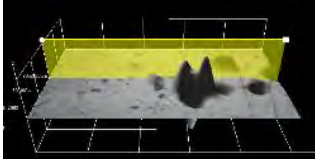

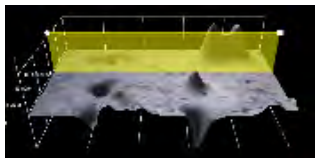
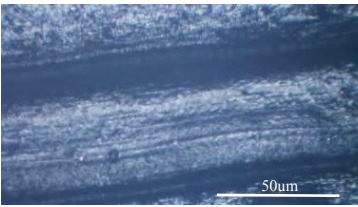
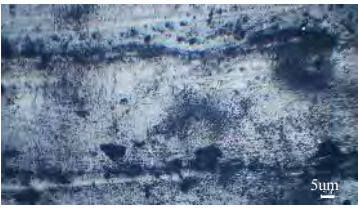
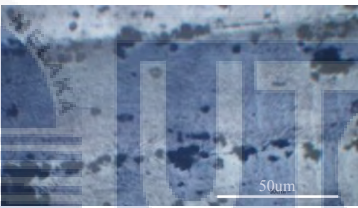

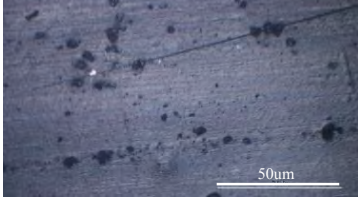
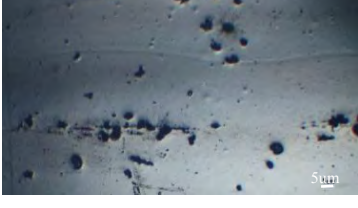

No	Exposure time (minutes)	Physical appearance	Surface Profile	Average surface roughness value, Ra (μm)
1	30			3.5945
2	60			2.8414
3	90			2.0716
4	120			1.1159
5	150			0.6448
6	180			0.2105
7	210			0.0990

Table 4.17: Optical Image of the Specimens (23.5 ml Acetone)

No	Exposure time (minutes)	Optical image, 5x magnifying lens	Average surface roughness value, Ra (μm)
1	0		4.4444
2	30		3.5945
3	60		2.8414
4	90		2.0716
5	120		1.1159
6	150		0.6448
7	180		0.2105

As shown in Table 4.17, the pattern lines formed during 3D printing process were gradually decreased when the acetone exposure time was increased. Therefore, by considering specimen's accuracy and prevent over-exposure happened, the optimal acetone exposure time was 180 minutes. However, the longer the acetone exposure time, the tensile strength of the specimen was slightly reduced.

4.5 Tensile Strength

Tensile stress test was performed to determine how much did the tensile strength in the specimens had reduced. According to ASTM D638 – 02a standard test method for tensile properties of plastics, this test method mainly used to determine the tensile properties of unreinforced and reinforced plastics in the form of standard dogbone-shaped test specimens when tested under defined conditions of pretreatment, temperature, humidity, and testing machine speed (ASTM International, 2004). This testing method only allow to test specimen with thickness up to 14mm. Tensile properties may provide useful data for conducting analysis in design purpose. However, due to high degree of sensitivities towards environmental condition, certain parameters condition need to be fixed before conducting this tensile stress experiment. The parameters condition to be fixed were listed in the Table 4.18 below. Figure 4.13 indicates the location of gauge length and grip length. Figure 4.14 demonstrates the universal testing machine to perform tensile strength test.

Table 4.18: Tensile Test Parameters Condition

Parameters	Description
Speed	5 mm/min
Gauge length, L_{Gauge}	50 mm
Grip length (each side), L_{Grip}	25 mm

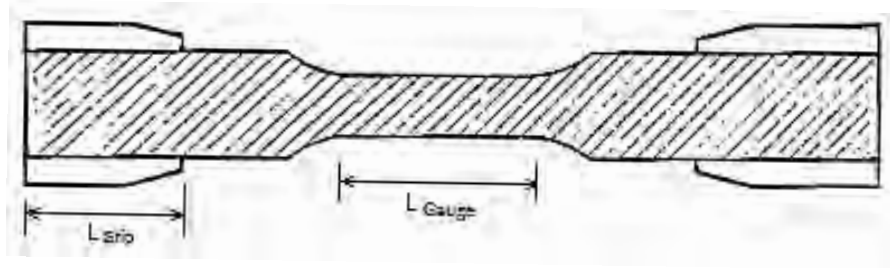


Figure 4.13: Tensile Test Specimen's Specification (ASTM International, 2004)

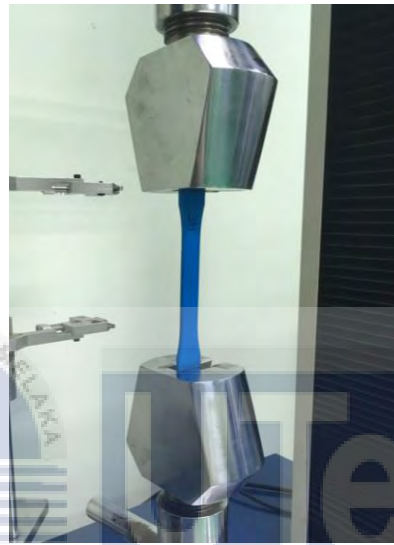


Figure 4.14: Universal Testing Machine

The tensile specimens were allowed to dry out for minimum 24 hours after Blow Cold vapor smoothing treatment to allow vapor on the surface was completely evaporated as the specimen was initially soft after the vapor smoothing treatment and was hardened after the vapor was fully evaporated. Table 4.19 below shows the result of tensile stress test for the specimens. Tensile strength of the material is defined as the maximum value of tensile stress of the material before the material rupture occurred. The maximum tensile strength of the specimen can be determined by measuring the peak value in the stress-strain curve. Figure 4.15 below shows the stress-strain curve for all the specimens and Figure 4.16 shows the relationship between exposure time and tensile strength of the specimens.

Table 4.19: Tensile Strength of the Specimens

Exposure time (minutes)	0	30	60	90	120	150	180
Tensile strength (MPa)	24.4457	22.4387	22.7953	19.5401	19.4329	19.8443	19.3664
Percentage of reduction	0%	8.21%	6.75%	20.07%	20.51%	18.82%	20.78%

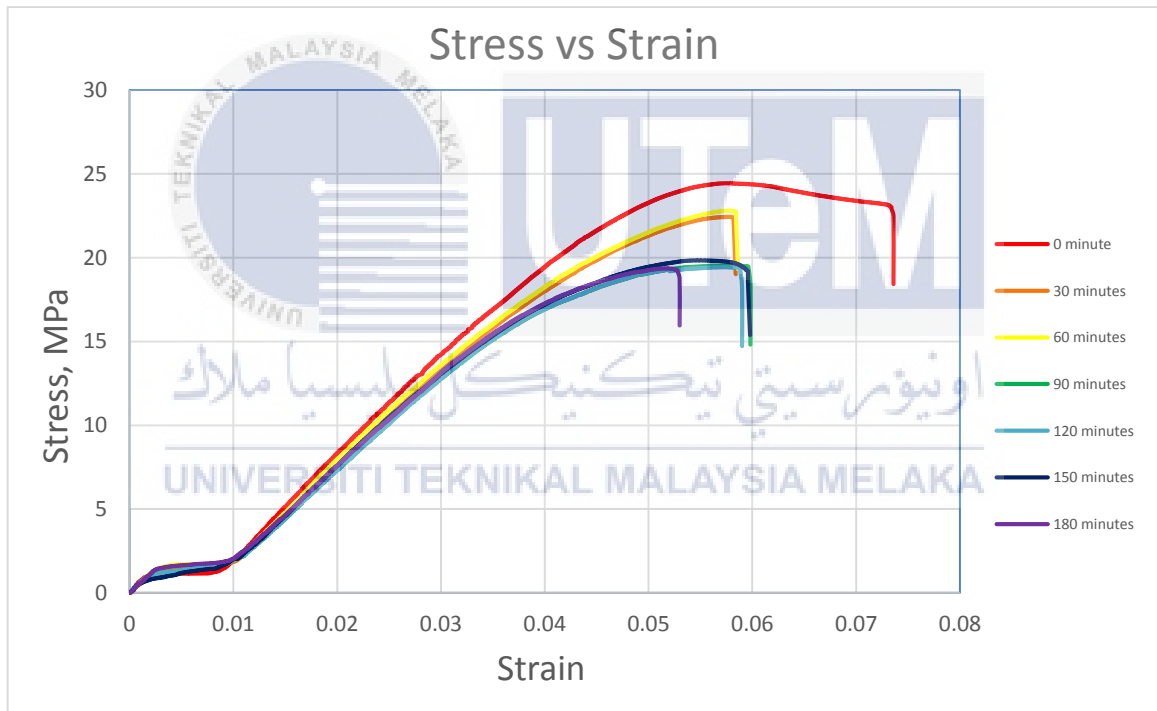


Figure 4.15: Stress – Strain Curve

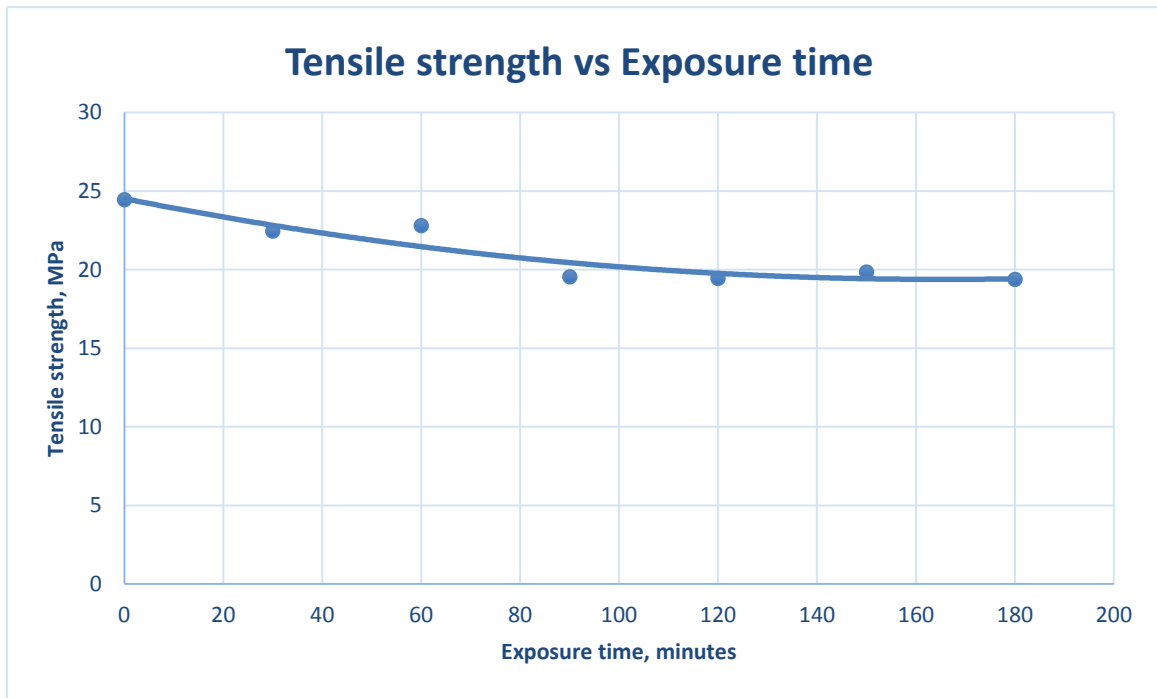


Figure 4.16: Graph of Tensile Strength against Exposure Time

Based on the observation in the graph of tensile strength against exposure time, the tensile strength of the specimen was slightly reduced as the acetone exposure time was increased. Previous research done by Galantucci (2010) found out that the surface roughness of the specimen was greatly reduced throughout the experiment with a minor reduction in tensile strength. The tensile strength of the treated specimen was reduced 17.7% in Galantucci's experiment. Research finding done by Mazlan (2018) found out that the tensile strength of the specimen was slightly linear decreased as the acetone exposure time was increased. The tensile strength obtained from Mazlan's experiment was reduced about 23.87% after the vapor smoothing treatment.

In this study, the result obtained was concurred with the previous result, which the tensile strength of the specimen was slightly decreased 20.78% after the Blow Cold vapor smoothing treatment. Tensile strength of the specimen decreased after the vapor smoothing treatment was due to the permanent chemical change occurred at the outermost surface of the specimen. Figure 4.17 shows cross section image of the specimen before treatment and

after treatment. Based on cross section image as shown in Figure 4.17, it clearly indicated that the acetone vapor has the chemical reaction towards the top surface of the specimen as shown in Figure 4.17b and did not penetrate deeply into the inner structure. The top three layers of the specimen was printed with 100 percent infill density, hence, it contributes the most towards the tensile strength for the specimen. As the acetone exposure time increases, it weakens the material structure of the top layer of the specimen, which results in decreasing its tensile strength.

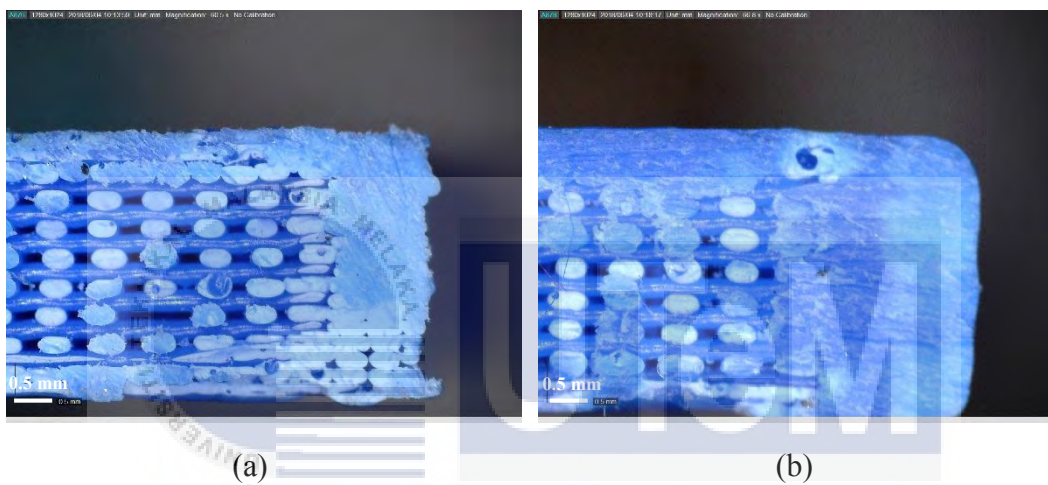


Figure 4.17: Cross Section of Dogbone Specimen. a) Before Treatment, b) After Treatment

UNIVERSITI TEKNIKAL MALAYSIA MELAKA

CHAPTER 5

CONCLUSION AND RECOMMENDATION

5.1 Justification of Objectives

There continues to be a problem in low cost Fused Deposition Modelling 3D printing technology related to surface roughness and staircase effect of the printed part. This study investigated the effectiveness of one of the post treatment process – Vapor smoothing. However, mechanical properties such as tensile strength and dimensional accuracy of the specimen got slightly affected throughout the process. This study also analyzed the amount of tensile strength in the specimen was reduced. In order to improve the surface roughness of the specimen and at the same time preserve its tensile strength and dimensional accuracy, an optimum vapor smoothing exposure time was studied.

5.2 Review of Methods

In this study, a new post treatment process was introduced, which was known as Blow Cold vapor smoothing treatment. This treatment process did not involve heating element and able to produce uniform surface finishing throughout the specimen. Unlike the previous research was done by heating the solvent in the enclosed chamber to produce solvent vapor and dispersed around the specimen. However, this method exposed the solvent to high temperature. In this case, solvent such as acetone is highly flammable and will cause explosion if do not handle with care. Another post treatment method discovered was known as Cold vapor smoothing technique, which involved soaking the wet towel with solvent and allowed it to slowly disperse the solvent vapor throughout the enclosed chamber. This

method ensures uniform surface finishing but extremely time-consuming. Besides that, acetone spraying technique also considered one of the post treatment process. This method is highly effective but produce inconsistent surface finishing.

The printing parameters involved in this study were layer thickness, infill density and nozzle temperature. An optimum printing parameter was studied to determine the lowest surface roughness value of the printed specimen using Taguchi method.

An enclosed glass container was fabricated to perform the Blow Cold vapor smoothing treatment. The specimens were underwent the Blow Cold vapor smoothing treatment in the interval of 30 minutes. The surface roughness value was measured using Shodensha GR3400 3D non-contact profilometer and the tensile strength test was performed using Shimadzu Ag-10kNX. The result of measured surface roughness value and tensile strength test were used to determine the optimum acetone vapor exposure time.

5.3 Review of Significant Findings

Taguchi results generated by Minitab 18.1 version showed that when layer thickness was 0.18, infill density was 60% and temperature was 225°C, it yielded the lowest surface roughness value, which was 3.37 μ m. The experiment continued by inserting the specimens into the Blow Cold vapor smoothing chamber with 23.5ml of acetone to be vaporized. It found that as the volume of the container increased, more amount of acetone was needed in order to produce the better surface finishing. As the acetone vapor exposure time increased, the surface roughness value was dramatically reduced to 95.26%, which was 0.2105 μ m. Besides that, it found that as the acetone vapor exposure time increased, the tensile strength of the specimen is slightly decreased from 24.4457 MPa to 19.3664 MPa, which was 20.78% reduced in tensile strength.

5.4 Explanation of Significance Findings

Based on the observation from the physical appearance on the surface of the untreated specimen, it noticed that the surface was getting rougher as the layer thickness increased from 0.18mm to 0.25mm and temperature increased from 210°C to 240°C. The bubble effect and burned marks were seen when temperature was increased to 240°C, which contributed the major effect towards surface roughness value of the specimen. However, as the temperature decreased to 210°C, inconsistent flow occurred which increased the surface roughness value.

Previous research had done Blow Cold vapor smoothing treatment using an enclosed chamber with the volume of 3610 cm³. The optimum acetone exposure time obtained was 3 hours, which reduced the surface roughness value to approximately 99% but reduce the tensile strength of the specimen by 23.87%. In this study, a new Blow Cold vapor treatment container was fabricated with the volume of 4250 cm³. Increased amount of acetone was needed in order to completely fill up the container with acetone vapor. As the acetone vapor exposure time increased, the surface roughness value was greatly reduced. It was due to the acetone vapor had sufficient time to completely react with the ABS material at the outermost surface of the specimen.

Besides that, the top three layers of the specimen was printed with 100% infill density, which contributed the most towards the tensile strength of the specimen. As the acetone vapor exposure time increased, a permanent chemical change occurred at the outer surface of the specimen, which weaken the material structure of the outer layer. This result in slightly decreased of the tensile strength in the specimen.

5.5 Limitation of the Study

This Blow Cold vapor treatment is only allow to treat for ABS material, as acetone is scientifically proven to be very effective solvent against ABS material. This post treatment process is mostly used in low cost Fused Deposition Modelling 3D printer. Low cost FDM 3D printer is proven that has the higher surface roughness value compared to other 3D printing techniques. Some automotive industries and bearing industries required to produce a frictionless product using low cost FDM 3D printer, hence, this study is suitable to reduce the surface roughness of the printed product.

5.6 Implications of the Study

This study introduces the new Blow Cold vapor smoothing treatment, which dramatically reduce the surface roughness value of the printed part. However, as the acetone vapor exposure time increases, the tensile strength of the printed part is slightly decreased.

5.7 Recommendations for Future Studies

Future study should investigate the post treatment for different type of materials such as PLA plastics. PLA printing material is cheaper and biodegradable than ABS material. Hence, PLA printing material is widely used in producing aesthetic products. However, PLA printing material has lower strength and durability compared to ABS material. Besides that, future study should investigate the size of the specimen that might affect the acetone vapor exposure time. In this study, the dogbone-shaped specimen is printed according to ASTM D638 standard Type I with the exposed surface area approximately 71.7592 cm². Increased in the specimen's exposed surface area might increase in the acetone vapor exposure time as more acetone vapor is required to react toward the larger surface of the specimen.

REFERENCES

- Antony, J., Warwood, S., Fernandes, K., & Rowlands, H. (2001). Process Optimisation Using Taguchi Methods of Experimental Design. *Work Study*, 50(2), 51–58. <https://doi.org/10.1108/00438020110366330>
- ASTM International. (2003). Standard Test Method for Tensile Properties of Plastics. *ASTM International*, 08, 46–58. <https://doi.org/10.1520/D0638-14.1>
- Babu, S. S., & Goodridge, R. (2015). Additive Manufacturing. *Materials Science and Technology*, 31(8), 881–883. <https://doi.org/10.1179/0267083615Z.000000000929>
- Bakar, N. S. A., Alkahari, M. R., & Boejang, H. (2010). Analysis on Fused Deposition Modelling Performance. *Journal of Zhejiang University*, 11(12), 972–977. <https://doi.org/10.1631/jzus.A1001365>
- Bharath Vasudevarao, B., Dharma Prakash Natarajan, D. P. ., & Henderson, M. (2000). Sensitivity of RP Surface Finish to Process Parameter Variation. *Solid Freeform Fabrication Proceedings*, 251–258. Retrieved from http://prism.asu.edu/publications/papers/paper00_srpsfppv.pdf
- Boschetto, A., & Bottini, L. (2014). Accuracy Prediction in Fused Deposition Modeling. *International Journal of Advanced Manufacturing Technology*, 73(5–8), 913–928. <https://doi.org/10.1007/s00170-014-5886-4>
- Campbell, I., Bourell, D., & Gibson, I. (2012). Additive Manufacturing: Rapid Prototyping Comes of Age. *Rapid Prototyping Journal*, 18(4), 255–258. <https://doi.org/10.1108/13552541211231563>

- Chaidas, D., Kitsakis, K., Kechagias, J., & Maropoulos, S. (2016). The Impact of Temperature Changing on Surface Roughness of FFF Process. In *IOP Conference Series: Materials Science and Engineering*, 161, pp. 1-8, Greece, 23-25 September 2016, Institute of West Macedonia. <https://doi.org/10.1088/1757-899X/161/1/012033>
- Comb, J. W., Priedeman, W. R., & Turley, P. W. (1994). FDM Technology Process Improvements. In: *Proceedings of the Solid Freeform Fabrication on 1994*, pp. 42–49, Austin, Texas, 8-10 August 1994, University of Texas
- David Thomas, S. (2003). Smoothing Method for Layered Deposition Modeling, United State of America, *US 8123999 B2*. Retrieved from <https://www.google.com/patents/US8123999>
- Dean, C. (2017). Design of Experiments (DOE) Tutorial. Retrieved from <http://asq.org/learn-about-quality/data-collection-analysis-tools/overview/design-of-experiments-tutorial.html> [Accessed on 12 December 2017]
- Dibya, C. (2017). STL File Format for 3D Printing. Retrieved from <https://all3dp.com/what-is-stl-file-format-extension-3d-printing/#pointone> [Accessed on 12 December 2017]
- Free Software Foundation. (2008). GNU Free Documentation License. Retrieved from <http://www.gnu.org/copyleft/fdl.html> [Accessed on 12 December 2017]
- Galantucci, L. M., Lavecchia, F., & Percoco, G. (2009). Experimental Study Aiming to Enhance The Surface Finish of Fused Deposition Modeled Parts. *CIRP Annals - Manufacturing Technology*, 58(1), 189–192. <https://doi.org/10.1016/j.cirp.2009.03.071>
- Galantucci, L. M., Lavecchia, F., & Percoco, G. (2010). Quantitative Analysis of A Chemical Treatment to Reduce Roughness of Parts Fabricated Using Fused Deposition

- Modeling. *CIRP Annals - Manufacturing Technology*, 59(1), 247–250. <https://doi.org/10.1016/j.cirp.2010.03.074>
- Gardan, J. (2015). Additive Manufacturing Technologies: State of The Art and Trends. *International Journal of Production Research*, 54(10), 1–15. <https://doi.org/10.1080/00207543.2015.1115909>
- Garg, A., Bhattacharya, A., & Batish, A. (2016). On Surface Finish and Dimensional Accuracy of FDM Parts after Cold Vapor Treatment. *Materials and Manufacturing Processes*, 31(4), 522–529. <https://doi.org/10.1080/10426914.2015.1070425>
- Guo, N., & Leu, M. C. (2013). Additive manufacturing: Technology, Applications and Research Needs. *Frontiers of Mechanical Engineering*, 8(3), 215-243. <https://doi.org/10.1007/s11465-013-0248-8>
- Gurr, M., & Mülhaupt, R. (2016). Rapid Prototyping. In *Polymer Science: A Comprehensive Reference*, 8(1), 77–99. <https://doi.org/10.1016/B978-0-444-53349-4.00202-8>
- Huang, S. H., Liu, P., Mokasdar, A., & Hou, L. (2013). Additive Manufacturing and Its Societal Impact: A Literature Review. *International Journal of Advanced Manufacturing Technology*, 67(5), 1191-1203. <https://doi.org/10.1007/s00170-012-4558-5>
- Huang, Y., Leu, M. C., Mazumder, J., & Donmez, A. (2015). Additive Manufacturing: Current State, Future Potential, Gaps and Needs, and Recommendations. *Journal of Manufacturing Science and Engineering*, 137(1). <https://doi.org/10.1115/1.4028725>
- Justin, S. (2017). 3D Modeling Software Produces Three-Dimensional Digital Effects. Retrieved from <https://www.lifewire.com/what-is-3d-modeling-2164>

- Kruth, J. P. (1991). Material Incess Manufacturing by Rapid Prototyping Techniques. *CIRP Annals - Manufacturing Technology*, 40(2), 603–614. [https://doi.org/10.1016/S0007-8506\(07\)61136-6](https://doi.org/10.1016/S0007-8506(07)61136-6)
- Lupulescu, N. B., Yordanova, S., & Mladenov, V., 2011. Paradigms of Total Quality Management. In Mandru, L., Patrascu, L., and Carstea, C., *Manufacturing Engineering, Quality and Production Systems*, Romania, 11-13 April 2011. Retrieved from https://www.researchgate.net/publication/275043929_Paradigms_of_Total_Quality_Management
- M. Johnson, W., Rowell, M., Deason, B., & Eubanks, M. (2014). Comparative Evaluation of An Open-Source FDM System. *Rapid Prototyping Journal*, 20(3), 205–214. <https://doi.org/10.1108/RPJ-06-2012-0058>
- M Nafis, O. Z., Nafrizuan, M. Y., Munira, M. A., & Kartina, J. (2012). Review on CNC-Rapid Prototyping. In *IOP Conference Series: Materials Science and Engineering* , 36, Pahang, 5-7 December 2011, <https://doi.org/10.1088/1757-899X/36/1/012032>
- Mazlan, Siti Nur Humaira; Alkahari, M. R., Ramli, F. R., & Maidin, N. A. (2018). Surface Finish and Mechanical Properties of FDM Part after Blow Cold Vapor Treatment. *Surface Finish and Mechanical Properties of FDM Part after Blow Cold Vapor Treatment*, pp. 1–5.
- Michael. (2015). Effect of Acetone Vapor Polishing on 3D Printed ABS Parts. Retrieved <https://engineerdog.com/2015/05/04/effect-of-acetone-vapor-polishing-on-3d-printed-abs-parts/> [Accessed on 12 December 2017]

- Minitab, I. (2017). What is the signal-to-noise ratio in a Taguchi design? Retrieved from <https://support.minitab.com/en-us/minitab/18/help-and-how-to/modeling-statistics/doe/supporting-topics/taguchi-designs/what-is-the-signal-to-noise-ratio/> [Accessed on 23 March 2018]
- Mitra, A. (2011). The Taguchi method. *Wiley Interdisciplinary Reviews: Computational Statistics*, 3(5), 472–480. <https://doi.org/10.1002/wics.169>
- Olivera, S., Muralidhara, H. B., Venkatesh, K., Gopalakrishna, K., & Vivek, C. S. (2016). Plating on Acrylonitrile–Butadiene–Styrene (ABS) Plastic: A Review. *Journal of Materials Science*, 51(8), 3657–3674. <https://doi.org/10.1007/s10853-015-9668-7>
- Open Source Hardware Association. (2017). Open Source Hardware (OSHW) Definition. Retrieved from <https://www.oshwa.org/definition/> [Accessed on 12 December 2017]
- Open Source Initiative. (n.d.). Basics of Open Source. Retrieved from <https://opensource.org/faq#osd> [Accessed on 12 December 2017]
- Osman Zahid, M. N., Case, K., & Watts, D. (2014). Optimization of Roughing Operations In CNC Machining for Rapid Manufacturing Processes. *Production and Manufacturing Research*, 2(1), 519–529. <https://doi.org/10.1080/21693277.2014.938277>
- Palermo, E. (2013). Fused Deposition Modeling: Most Common 3D Printing Method. Retrieved from <https://www.livescience.com/39810-fused-deposition-modeling.html> [Accessed on 29 May 2018]
- Pandey, P. M., Reddy, N. V., & Dhande, S. G. (2003). Improvement of Surface Finish by Staircase Machining in Fused Deposition Modeling. *Journal of Materials Processing Technology*, 132(1–3), 323–331. [https://doi.org/10.1016/S0924-0136\(02\)00953-6](https://doi.org/10.1016/S0924-0136(02)00953-6)

- Pham, D., & Gault, R. (1998). A Comparison of Rapid Prototyping Technologies. *International Journal of Machine Tools and Manufacture*, 38(10–11), 1257–1287. [https://doi.org/10.1016/S0890-6955\(97\)00137-5](https://doi.org/10.1016/S0890-6955(97)00137-5)
- Rao, A. S., Dharap, M., Venkatesh, J., & Ojha, D. (2012). Investigation of Post Processing Techniques To Reduce the Surface Roughness of Fused Deposition Modeled Parts, *International Journal of Mechanical Engineering and Technology*, 3(3), 531-544.
- Reprap.org. (2017). RepRapWiki. Retrieved from <http://reprap.org/wiki/About> [Accessed on 12 December 2017]
- Sean, R. (2017). PLA vs ABS: Filaments for 3D Printing Explained and Compared. Retrieved from <https://all3dp.com/pla-abs-3d-printer-filaments-compared/> [Accessed on 12 December 2017]
- Sells, E., Bailard, S., Smith, Z., Bowyer, A., & Olliver, V. (2009). RepRap: The Replicating Rapid Prototyper: Maximizing Customizability by Breeding the Means of Production, *Handbook of Research in Mass Customization and Personalization*, World Scientific Publishing Company, 1, pp. 568–580. https://doi.org/10.1142/9789814280280_0028
- Statsoft (2017). Statistica Help Taguchi Methods: Robust Design Experiments Signal-to-Noise (S/N) Ratios. Retrieved from <http://documentation.statsoft.com/STATISTICA Help.aspx?path=Experimental/Doe/Overview/TaguchiMethodsSignaltoNoiseSNRatios> [Accessed on 14 May 2018]
- Sundararajan, K. (2000). Design of Experiments. Retrieved from <https://www.isixsigma.com/tools-templates/design-of-experiments-doe/design-experiments-primer/> [Accessed on 26 December 2017]

ThomasNet. (2017). Introduction to G-code. Retrieved from <https://www.thomasnet.com/articles/custom-manufacturing-fabricating/introduction-gcode/> [Accessed on 12 May 2018]

Wittbrodt, B. T., Glover, A. G., Laureto, J., Anzalone, G. C., Oppliger, D., Irwin, J. L., & Pearce, J. M. (2013). Life-Cycle Economic Analysis of Distributed Manufacturing with Open-Source 3-D Printers. *Mechatronics*, 23(6), 713–726. <https://doi.org/10.1016/j.mechatronics.2013.06.002>

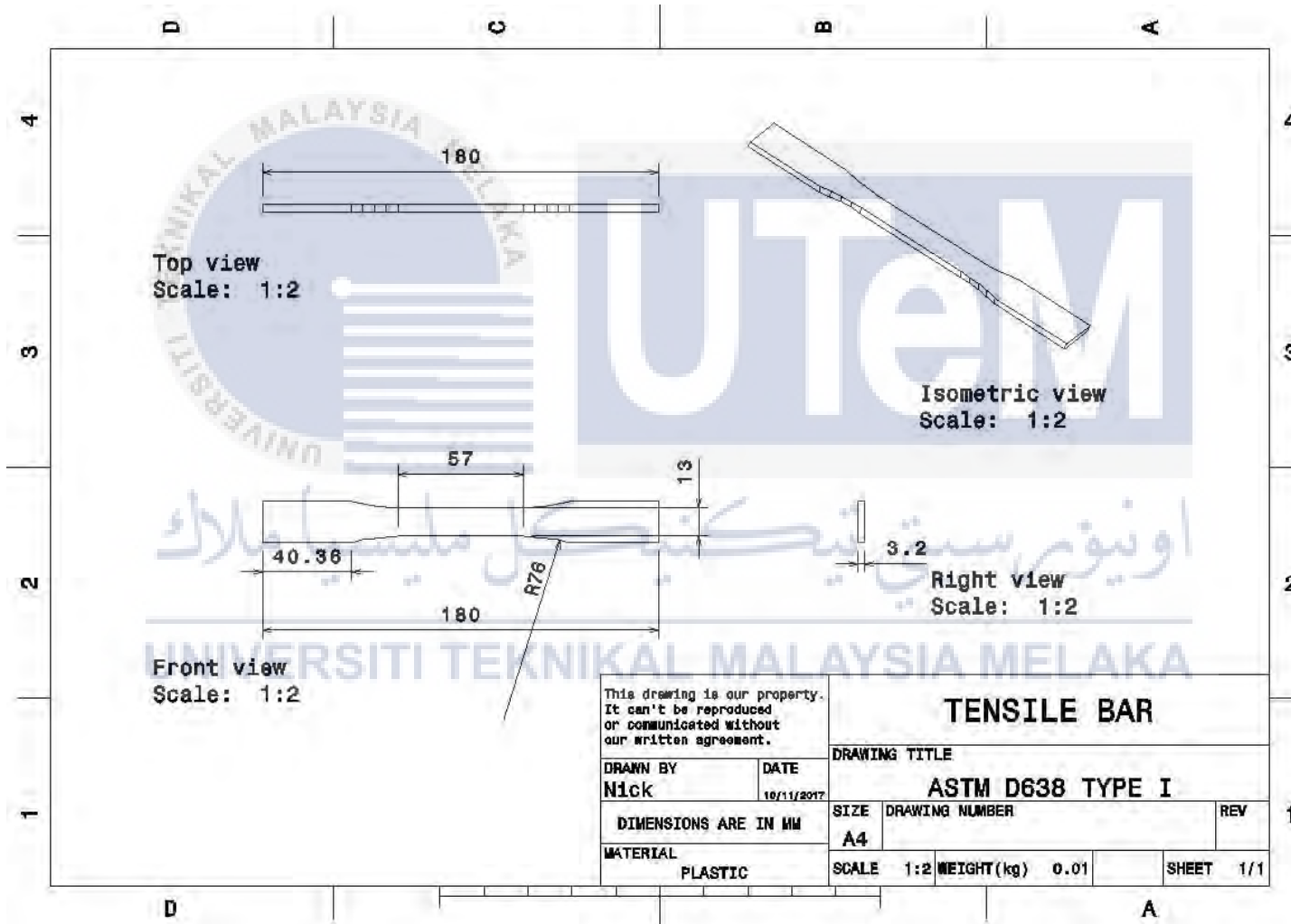
Yan, X., & Gu, P. (1996). A Review of Rapid Prototyping Technologies and Systems. *CAD Computer Aided Design*, 28(4), 307-318. [https://doi.org/10.1016/0010-4485\(95\)00035-6](https://doi.org/10.1016/0010-4485(95)00035-6)

Yang, K., & El-Haik, B. (2008). Taguchi's Orthogonal Array Experiment, *Design for Six Sigma: A Roadmap for Product Development*. Retrieved from <http://www.weibull.com/hotwire/issue131/hottopics131.htm> [Accessed on 12 May 2018]

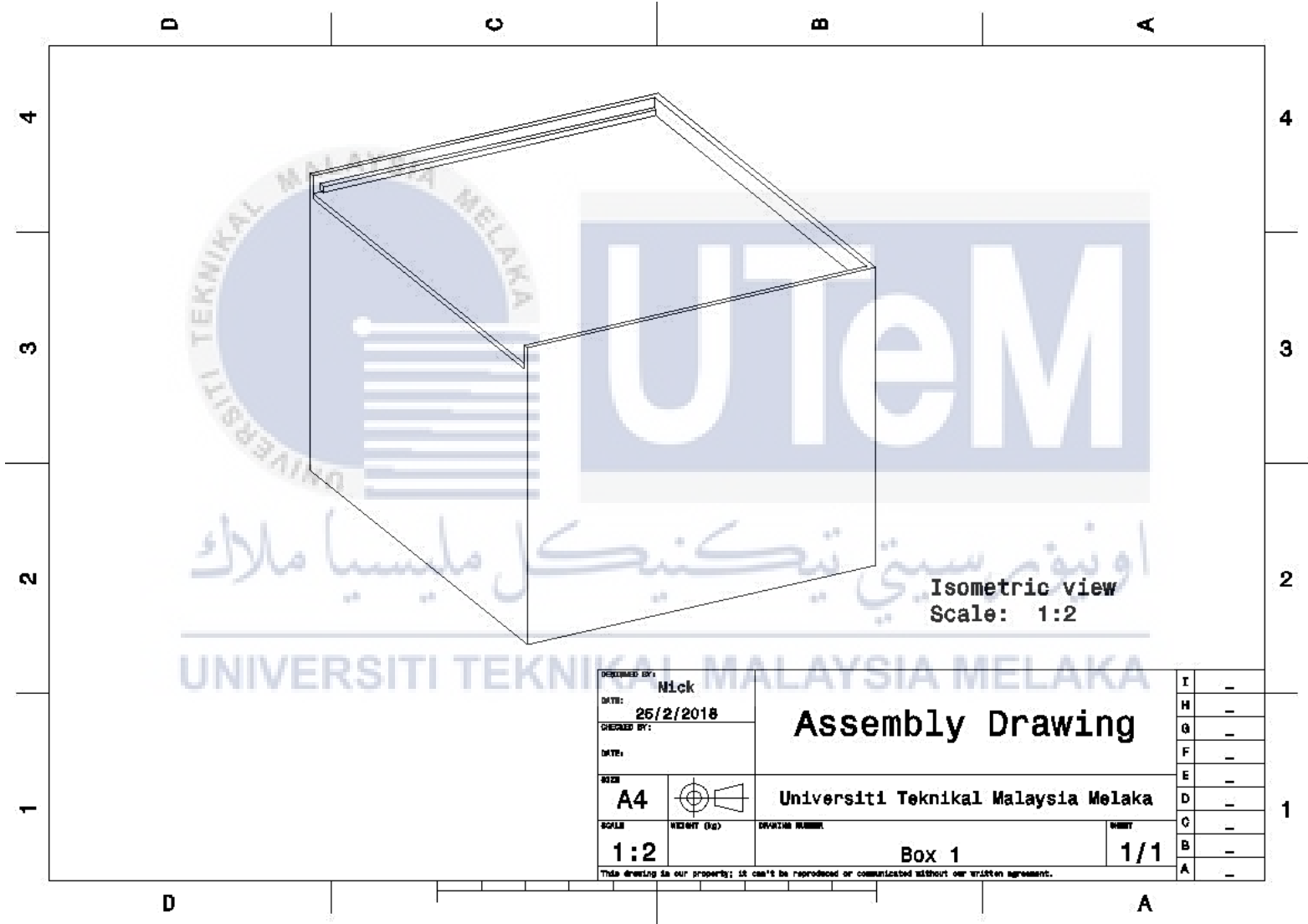


APPENDICES

A. SPECIMEN DIMENSION ASTM D368 TYPE I

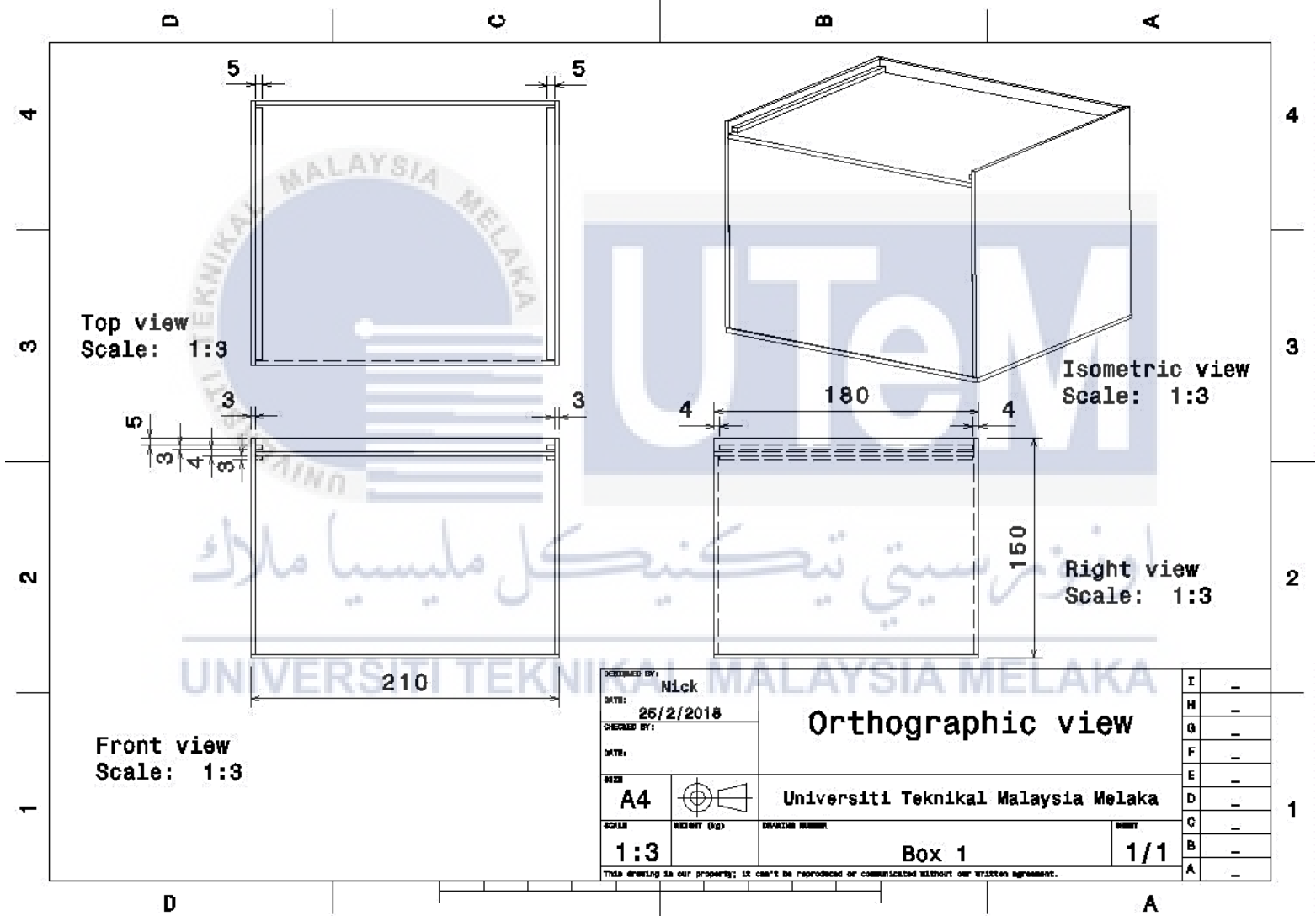


B. BLOW COLD VAPOR SMOOTHING TREATMENT CHAMBER ASSEMBLY DRAWING

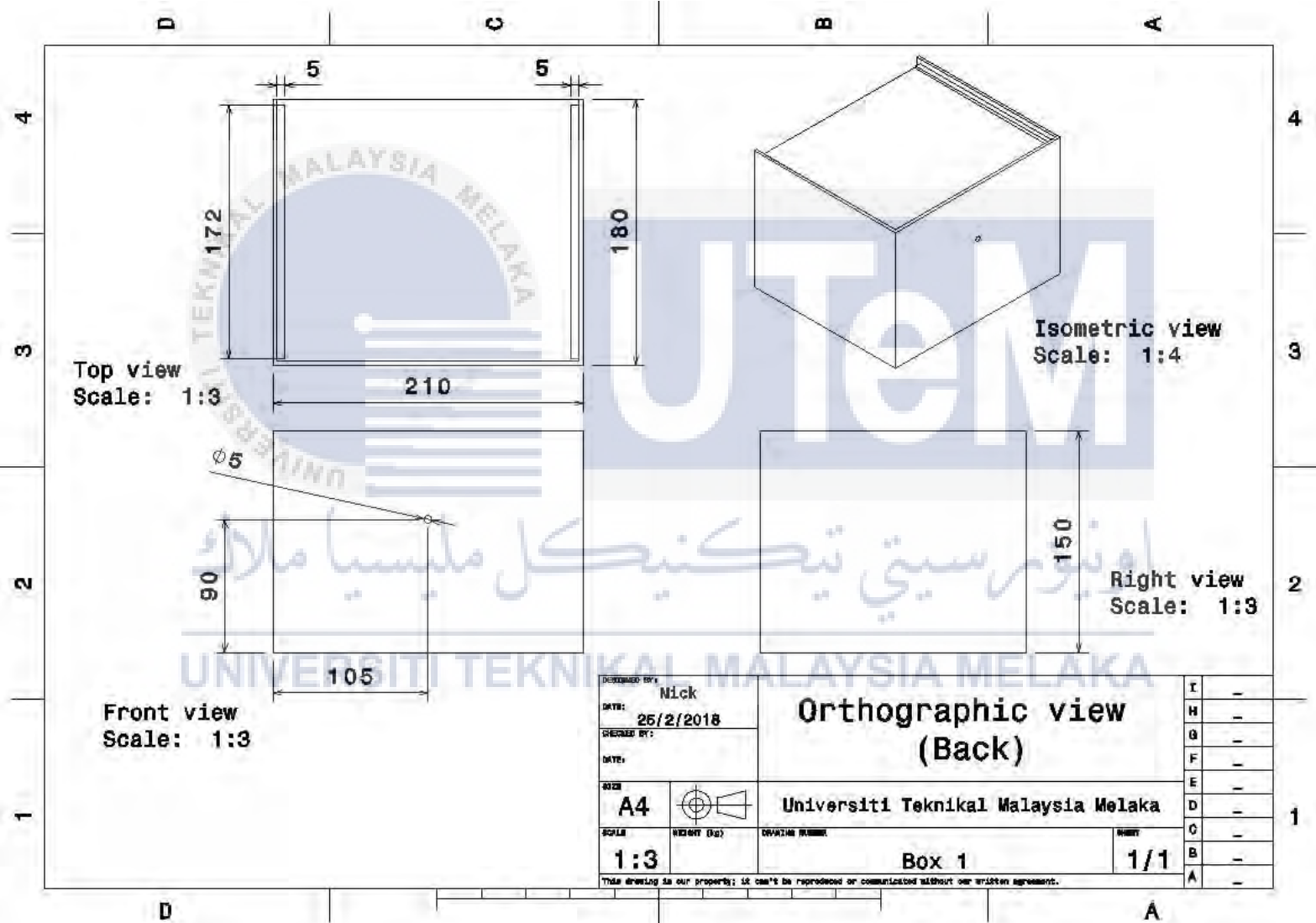


DESIGNED BY: Nick		Assembly Drawing	I	-
DATE: 26/2/2018			H	-
CHECKED BY:			G	-
DATE:		F	-	
SIZE: A4		Universiti Teknikal Malaysia Melaka	E	-
SCALE: 1:2			D	-
WEIGHT (kg):		C	-	
DRAWING NUMBER: Box 1		B	-	
SHEET: 1/1		A	-	

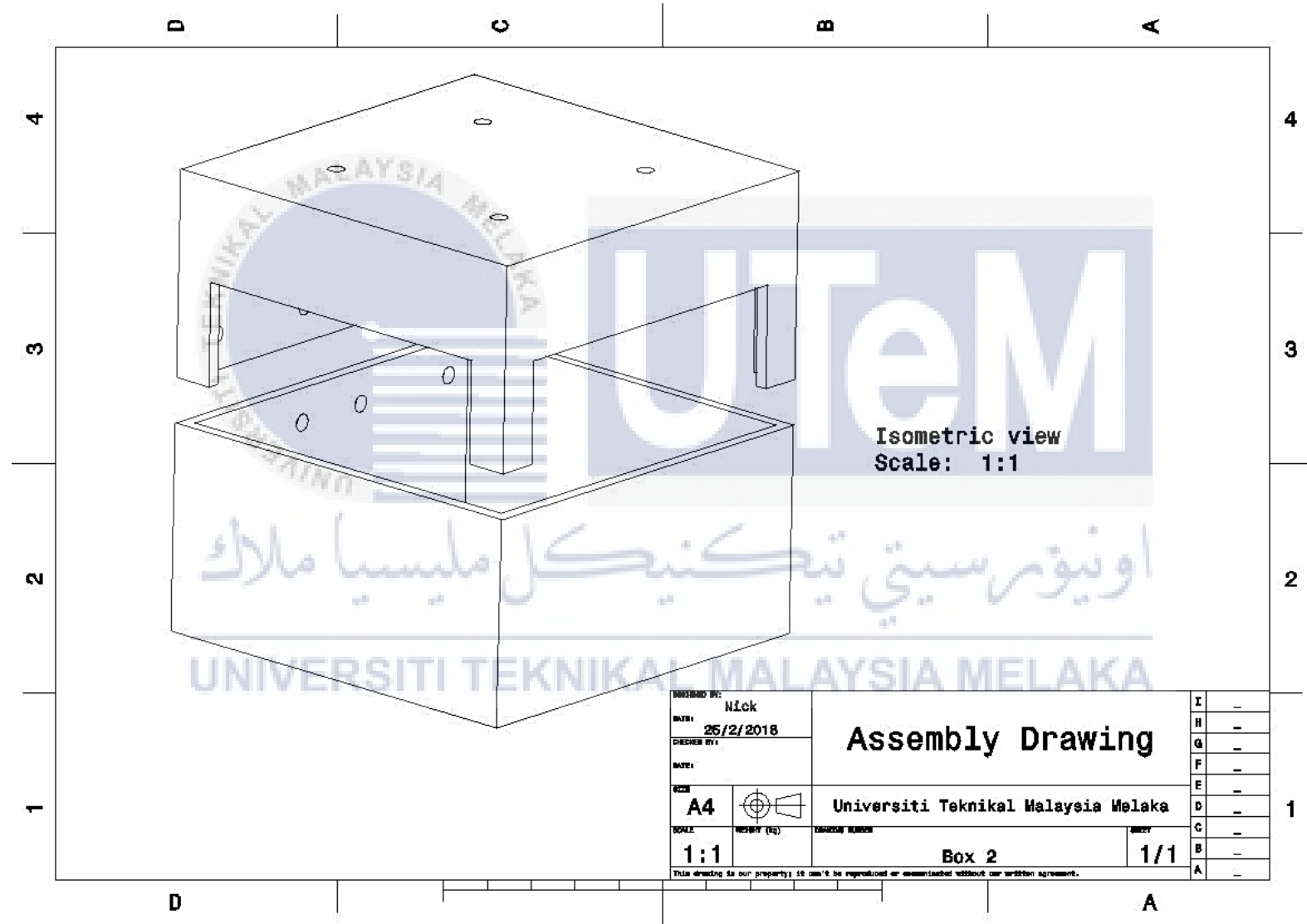
C. BLOW COLD VAPOR SMOOTHING TREATMENT CHAMBER ORTHOGRAPHIC DRAWING (FRONT SIDE)



D. BLOW COLD VAPOR SMOOTHING TREATMENT CHAMBER ORTHOGRAPHIC DRAWING (BACK SIDE)

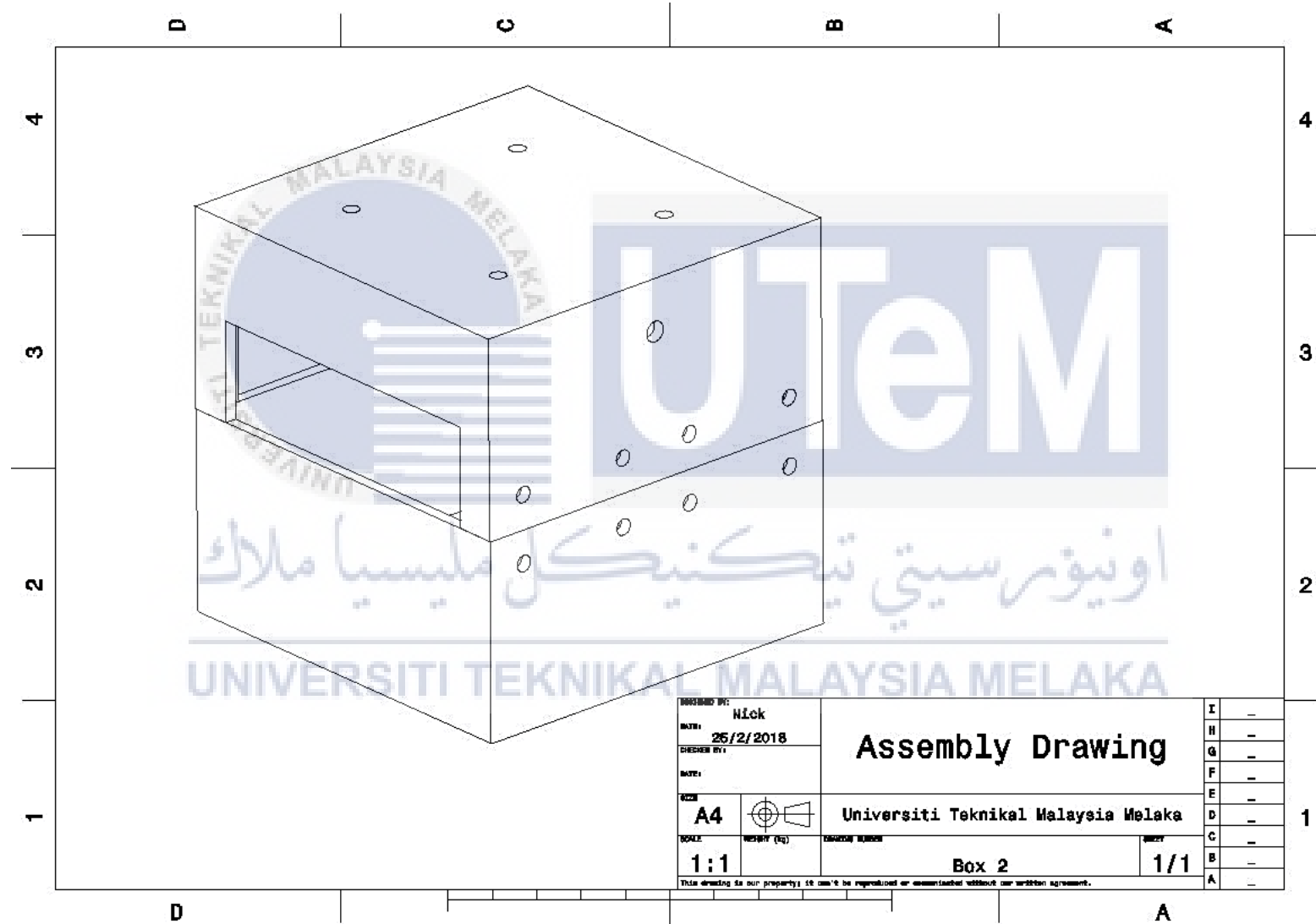


E. ACETONE CONTAINER ASSEMBLY DRAWING (FRONT SIDE)



DRAWN BY: Nick		Assembly Drawing	I	-
DATE: 26/2/2018			H	-
CHECKED BY:		G	-	
DATE:		F	-	
SIZE: A4		E	-	
SCALE: 1:1		D	-	
DESIGN NUMBER: Box 2	UNIVERSITI TEKNIKAL MALAYSIA MELAKA	C	-	
		B	-	
		A	-	

F. ACETONE CONTAINER ASSEMBLY DRAWING (BACK SIDE)



G. ACETONE CONTAINER ORTHOGRAPHY VIEW

